School of Graduate Studies

College of Social Science

Department of Geography and Environmental Studies

Spatio-Temporal Patterns of NDVI in Response to Rainfall Variability by Using Remote Sensing Approaches in Drought-Prone Area of Awash Basin, Ethiopia.

BY

DEMBEL BONTA GEBEYEHU

A Thesis Submitted to the School of Graduate Studies of Addis Ababa University in partial fulfillment of the requirement for the Degree of Master of Arts in Geography and Environmental Studies Specialization in Geographic Information System (GIS), Remote Sensing (RS), and Digital Cartography

Addis Ababa University

Addis Ababa, Ethiopia

June, 2017

Spatio-Temporal Patterns of NDVI Response to Rainfall Variability by Using Remote Sensing Approaches in Drought-Prone Area of Awash Basin, Ethiopia.

By

DembelBontaGebeyehu

A Thesis Submitted to the School of Graduate Studies of Addis Ababa University in partial fulfillment of the requirement for the Degree of Master of Arts in Geography and Environmental Studies Specialization in Geographic Information System (GIS), Remote Sensing (RS), and Digital Cartography

Under the Supervision of

ErmiasTeferi (PhD)

Assistant professor

Chair Person of Center for Environmental Studies

College of Development Studies Addis Ababa University

Addis Ababa Ethiopia

Addis Ababa Ethiopia

June, 2017

Addis Ababa University

School of Graduate Studies

This is to certify that the thesis prepared by DEMBEL BONTA GEBEYEHU, titled with Spatio-Temporal Patterns of NDVI Response to Rainfall Variability by Using Remote Sensing Approaches in Drought-Prone Area of Awash Basin, Ethiopia and submitted in partial fulfillment of the requirements for the Degree of Master of Arts in GIS, Remote Sensing, and Digital Cartography complies with the regulations of the university and meets the accepted standards with respect to the originality and quality.

Approved by the Examining Committee:

Internal Examiner: Dr. Aragaw Alemayehu Signature _____Date_____

External Examiner: Dr. Berhan Gessesse Signature _____Date_____

Advisor: Dr. Ermias Teferi Signature _____Date_____

Chairman, Department

Dr. Tebarek Lika Signature _____Date_____

Acknowledgement

It is with great pleasure to thank my advisor Dr. Ermias Teferi for his scholarly support and supervision in all aspects and framework of the research. He was not just only my advisor but also my mentor for my future carrier as well as to be equipped with all disciplinary ethics, commitment and knowledge. Without him many improvements in this research work could not be possible. Thank you sir for all.

I express my sincere gratitude to all the team members of NASA NOAA-AVHRR Global Inventory Modeling and Mapping Studies (GIMMS) NDVI3g Group, in particular Campton J. Tucker and Jorge E. Pinzon for more than 30 years commitment in processing and continuous improvements of global NDVI data, which is the only long term historical global NDVI data. I am also thankful for all the TAMSAT research group members at the department of Meteorology University of Reading.

My special acknowledgement is also for the members of Clark Labs, Clark University; particularly J. Ronald Eastman, for their sharing of actual demo (one month free trial period of all versions). My special thanks to the Ministry of Environment, Forestry and Climate Change (MEFCC) and United Nations Food and Agricultural Organization (UN-FAO), especially Ato Melakneh Delet and Ato Asaye Nigusie for their sharing of land cover land use data that was produced by joint project between UN-FAO and MEFCC.

I am grateful for all staff members of department of geography and environmental studies of Addis Ababa University. Finally, I extend my appreciation for Sadnur Werku for his technical and moral support.

Dembel Bonta

Table of Contents

Content **Page**

List of Tables

Page No.

List of Figures

Page No.

Acronym

ABA	Awash Basin Authority
AVHR	Advanced Very High Resolution Radiometer
CCD	Cold Cloud Duration
CSA	Central Statistics Agency
CV	Coefficient of Variation
ESRI	Environmental System Research Institute
EUMETSAT	European Organization for the Exploitation of Meteorological Satellites
GIMMS	Global Inventory Modeling and Mapping Studies
GIS	Geographical Information System
IPCC	Inter-Governmental Panel on Climate Change
MEFCC	Ministry of Environment, Forestry and Climate Change
Meteosat	Meteorological Satellite
MODIS	MODerate resolution Imaging Spectro-radiometer
MVC	Maximum Value Composite
NASA	National Aeronautics and Space Administration
NDVI3g	Normalized Difference Vegetation Index third Generation
NOAA	National Oceanic and Atmospheric Administration-
RFE	Rainfall Estimates
RS	Remote Sensing
TAMSAT	Tropical Application of Meteorology using SATellite and Ground Rain gauge
TRMM	Tropical Rainfall Measuring Mission
UN-FAO	United Nations Food and Agricultural Organization
UNFCC	United Nations Framework Convention on Climate Change

Abstract

Global and local rainfall variability and change has a great impact on vegetation dynamics at spatial and temporal scales. This study was conducted with the main aim to assess the spatio-temporal patterns of vegetation and rainfall as well as vegetation response to rainfall variability by incorporating satellite-derived vegetation index and rainfall estimate for the period of 30 years from 1983 – 2012 in the Awash basin, Ethiopia. Two satellite derived data have been used; a non-stationary satellite 15-day MVC GIMMS NDVI3g time series data onboard of NOAA-AVHRR and monthly TAMSAT RFE v2 of the Metosat satellite data were obtained and processed to achieve the stated objective. Two types of long term inter-annual trend analysis i.e. monotonic trend analysis and linear trend (Theil-Sen slope estimator) as well as one trend significance test (Mann-Kendal significance test Z-score) has been performed on both NDVI3g and RFE. Similarly, Harmonic analysis and Thiel-Sen slope estimator have been used to assess the seasonal trend analysis of NDVI and rainfall in the study area for the studied 30 years period (1983 – 2012). Likewise, linear modeling has been also employed to investigate the response of vegetation to rainfall variability from 1983 – 2012 in the Awash basin. The results from inter-annual trend analysis showed that, the major vegetation classes revealed a decreasing trends and increasing trends of rainfall with different significant percentage in the whole basin as well as for different major land cover types. On the other hand, the seasonal patterns and trends also showed an increasing trend of rainfall and vegetation in the study area. The correlation between vegetation responses to rainfall was 30 days lag (lag1) for short term lag relationship; and below 30 days (lag0) is for long term inter-annual lag relationship. Therefore, the findings of this study can be used for early warning system like drought forecasting.

Key words: NDVI3g, Time series trend analysis, Rainfall variability, Mann-Kendal, Theil-Sen Slope

CHAPTER ONE

INTRODUCTION

1.1.Background of the Study

Global and local rainfall variability and change have a great impact on vegetation dynamics at spatial and temporal scales, where they are important constituents of the global ecosystem. In this regard, vegetation controls global ecosystem through terrestrial soil stability, atmospheric circulation, and hydrological retention. It also helps to maintain a balance of an ecosystem. Studies indicated that there is a direct relationship between climate change/variability, in particular, precipitation, and vegetation (e.g. Anyamba and Tucker, 2005; Vrieling et al., 2011) Therefore, it is important to monitor the relationship between vegetation and rainfall (Zhong et al., 2010).

Vegetation growth and development have been monitored by using satellite remote sensing since inception of remote sensing (Rembold et al., 2013). Satellite-derived measurements from vegetation canopy absorption and reflection properties in the visible and infrared magnetic spectrum are known as vegetation indices/VIs/, can provide information about the vegetation status. From the different VIs, Normalized Difference Vegetation Index (NDVI) by Rouse et al., in 1974 (Deering, 1978), used most often to study vegetation greenness, stress, health and crop production (Tucker et al., 1980; Sellers, 1985; Vrieling et al., 2011).

Several studies have assessed the relationship between vegetation and climate, particularly with temperature and precipitation at global and regional scales (e.g.Zhang et al., 2005; Martiny et al., 2006; Leilei et al., 2014). A strong correlation between vegetation response and rainfall was obtained at global and continental level (Zhang et al., 2005). Similarly, in several areas of Africa a significant correlation between rainfall and NDVI was reported (Martiny et al., 2006). Other studies also revealed that, direct relationship was observed during the good rainfall season and peak of NDVI, the correlation between vegetation and precipitation is higher than temperature in Tibetan plateau (Mingjun et al., 2007; Leilei et al., 2014); their relationship is strong and predictable when viewed at the appropriate spatial scale in central great plains of USA (Wang et al., 2003).

On the other hand, a review in the works of Chamaille and Fritz (2009) indicated that different areas have shown a weak relationship between precipitation and vegetation, particularly in the long term annual /inter-annual/ scale. Another finding by Fang et al., (2001) there is a weak relationship between precipitation and vegetation but a significant relationship.

Therefore, this study has been conducted on the spatio-temporal patterns of NDVI and rainfall as well as the relationship between NDVI in response to rainfall variability from 1983 to 2012 by using time series analysis in the Awash Basin, Ethiopia.

1.2.Statement of the Problem

Rainfall variability has different catastrophic consequences in many parts of developing countries like Ethiopia. On the other hand, rainfall intensity and periodicity within a season or year to year has a great impact on the livelihoods system of households and natural resources. The majority parts of the basin have short and intense rainy seasons with highly unreliable rainfall leading to frequent droughts and floods in the middle and lower parts of the basin. Rainfed cultivation and natural vegetation, as well as livestock fodder supply, have increasingly becoming unreliable in the larger lower part of the basin (Awash Basin Authority (ABA), 2017). In the same way, there is also forest degradation in the Awash basin resulted from different anthropogenic processes. Similarly, rainfall is extremely variable in both space and time have and reoccurring water shocks, such as drought and flood can have considerable social and economic impacts. Good predictions depend on a secure knowledge of present rainfall - but this is poorly understood due to the inadequacy of ground-based observations. In other words, satellite-based rainfall estimate can be used to fill the gap (Maidment et al., 2014). Therefore, the presence of trends by conducting the spatio-temporal trends of rainfall and vegetation, and the response of vegetation to rainfall variability as well as the relationship between rainfall and different types of vegetation through time series trend analysis and linear modeling will help to identify and inform the stakeholders to take peculiar measures. Owing the above facts, this study was conducted.

Moreover, the spatio-temporal patterns of vegetation change or land cover land use change may occur either through gradual change or abrupt shift at a specific point in time (Donald et al., 2011). Those changes have been studied through change detection strategies. This strategy was

developed in the period of image scarcity by focusing on comparing a few scenes (Jensen, 1996). Image time series that is taken over continuous time period has an advantage of getting sufficient temporal scenes in terms of duration and frequency; consequently allows detection of changes of substantial and abrupt variation that are not possible to detect in the traditional approaches of change detection (Beurs & Henerbry, 2005). Thus, this study has been conducted on the spatial and temporal patterns of NDVI in response to rainfall variability from 1983 to 2012 by using time series trend analysis and linear modeling in the Awash Basin, Ethiopia.

Besides, the existing studies undertaken in Ethiopia as well as in the study area were limited in their area of interest. Getahun (2012) investigated the spatio-tempotal pattern of precipitation and the response of vegetation to precipitation in Ethiopia from 1996 to 2008 (12 years). To achieve the stated objective NDVI and rainfall estimates from the National Oceanic and Atmospheric Administration (NOAA) satellites were used; whereas different land cover classes were derived from the Global Land Cover Network (GLCN). The study also employed Pearson's correlation coefficient to estimate the lag relationship between NDVI and rainfall. The findings of the study showed that, vegetation responded directly to precipitation and the seasonal patterns also showed 0 to 3 months lag between precipitation and vegetation.

Another study was undertaken by using NOAA AVHRR NDVI and observed rainfall data at climate stations to monitor desertification processes through NDVI and rainfall trends over time from 1982-2006 in Ethiopia (Gezahegn Negash, 2016). Linear regression has been validated using vegetation trends as a proxy for degradation processes. Furthermore, the discussion was conducted based on 25 selected climate stations for the entire country. The findings of the study indicated that, majority of the stations have no trends of NDVI and rainfall and strong relationship between NDVI and rainfall at station level.

On the other hand, Teferi et al., (2015), have conducted inter-annual and seasonal trends of vegetation in the Upper Blue Nile of Ethiopia by using GIMMS NDVI (1981 – 2006) and MODIS NDVI (2001 – 2011). The proposed and employed methodology in Teferi et al. (2015) was harmonic analyses and non-parametric trend tests. The results from inter-annual trend of GIMMS NDVI showed around 77 % have positive trends and out of this 41.15 % have showed significant increases. However, the results from MODIS NDVI about 36 % of the basin showed decreasing trends. Moreover, the seasonal trend analysis indicated that, over half of the Abay

Basin (particularly, shrubland and woodland vegetation classes) found to exhibit significant trends in seasonality over the 25-year period (1982–2006).

Likewise, studies undertaken in the Awash basin dealt with different aspects of drought which is related with erratic rainfall. A study by Desalegn et al., (2006), to analyze drought characteristics based on meteorological and hydrological variables in the Awash River Basin of Ethiopia. Standardized precipitation index was used for temporal and spatial analyses of meteorological drought. The results of the study indicate that, extreme drought category on 12-month time scale indicated that extreme events occur most frequently in the Upper and Middle Awash Basin; while considering the overall categories of drought, the most frequent droughts occurred in the Middle and Lower Awash Basin during the period of analysis. Similarly, results based on hydrological drought analysis shows that the severest drought events occurred in the Middle Awash Basin during May 1988 to June 1988 and April 1998 to May 1998.

Correspondingly, Belayneh et al. (2013) conducted a study to assess long-term drought forecasting in Awash River Basin of Ethiopia. The study compared the effectiveness of five data driven models for forecasting long-term (6 and 12 months lead time) drought conditions in the study area. The Standard Precipitation Index (SPI 12 and SPI 24) was forecasted using a traditional stochastic model (ARIMA) and compared to machine learning techniques i.e. artificial neural networks (ANNs) and support vector regression (SVR). The forecast results indicated that, the coupled wavelet neural network (WA-ANN) models were better than all the other models in this study for forecasting SPI 12 and SPI 24 values over lead times of 6 and 12 months in the Awash River Basin.

However, there is lack of empirical researches that has been conducted to assess the long-term trends and relationship between rainfall variability and vegetation using GIMMS NDVI3g and RFE data sets for the Awash River Basin of Ethiopia. This thesis hypothesizes that the new geospatial datasets will provide us new evidence about the relationship between rainfall variability and vegetation development. Therefore, the present study has been conducted to assess the spatial and temporal patterns of vegetation in response to rainfall variability by using satellite derived TAMSAT rainfall estimate version two (RFE-V2) and GIMMS NDVI3g time series from 1983 to 2012 for the entire Awash basin in Ethiopia.

1.3.Objective of the Study

1.3.1. General Objective of the Study

The general objective of the study was to assess the spatio-temporal trends of vegetation and rainfall as well as the relationship between vegetation and rainfall variability by integrating GIMMS NDVI3g and TAMSAT RFE from 1983 to 2012 for the entire Awash basin in Ethiopia.

1.3.2. Specific Objectives of the Study

The specific objectives of this thesis were;

- To analyze the inter-annual trends of vegetation and rainfall over the study period from 1983 to 2012 in Awash Basin Ethiopia;
- To analyze the seasonal trends of vegetation and rainfall variability throughout 30 years of period in the study area; and
- To evaluate the relationship between vegetation in response to rainfall variability by incorporating satellite-derived RFE and GIMMS NDVI3g in the study area;

1.4.Research Questions

The project has tried to address the following questions;

I. What is the inter-annual trend of vegetation and rainfall over the study period from 1983 to 2012 in Awash Basin Ethiopia?
II. What is the seasonal trend of vegetation and rainfall variability throughout 30 years of the period in the study area?; and
III. What is the relationship between vegetation in response to rainfall variability in the study area?

1.5.Significance of the Study

The results of the study from the new data sets of the third generation vegetation index i.e. GIMMS NDVI3g, and the newly calibrated TAMSAT RFE V2 will add knowledge on the present academics about the long-term trends of vegetation and rainfall as well as the relationship between vegetation in response to rainfall variability over the period from 1983 to 2012 in the Awash basin, Ethiopia. It will also help as a reference for further researches in the areas of time series trend analysis for inter-annual and seasonal trends of vegetation and rainfall as well as the response of vegetation index to rainfall variability in other parts of river basins of the world in general and the study area in particular.

The findings of the study will inform the stakeholders about the trends of different types of vegetation and rainfall over the study period of 30 years and the relationship between vegetation in response to rainfall variability. This would have enormous significance for the stakeholders in devising peculiar circumstances and implementing case specific intervention plans.

1.6.Scope of the Study

The study was conducted in one of the river basins found in Ethiopia i.e. Awash River Basin. The study does not provide an exhaustive account of satellite remote sensing application for analyzing vegetation in response to rainfall variability in other river basins of Ethiopia. Similarly, it focused on the inter-annual and seasonal trends of vegetation and rainfall as well as the spatial and temporal response of major vegetation types of land cover land use (by focusing on agricultural land, grassland, shrublands, bareland, dense woodland and forest) to rainfall variability over the period of 1983 to 2012.

1.7.Limitation of the Study

There are also other different factors for vegetation growth and development and response of vegetation include; temperature, soil characteristics, topography (slope and aspect), and human factors. However, the study was conducted only by taking rainfall as a factor for vegetation dynamics. In the same vein, the start, length, peak and end of rainfall may correspond to some months, particularly during the rainy months (season). The seasonal analysis was conducted on the assumption of two seasons within a year.

1.8.Organization of the Paper

The research project contains five chapters. The first chapter introduces the study. Chapter two discusses the related concepts and empirical literatures. Description of the study area and research methodology has been presented in the third chapter. Chapter four dealt with the results and discussion of the study. The conclusion was made and recommendations have been forwarded on the fifth chapter.

CHAPTER TWO

REVIEW OF RELATED LITERATURE

2.1. Spatio-Temporal Patterns and Variability of Rainfall and Vegetation

From the theoretical perspectives, there are three types of rainfall variability (NEST, 2003). The first one, spatiotemporal rainfall variability, is the differences in the total rainfall received between places structurally located within a given region over a period of time. The second is inter-annual rainfall variability, is the annual deviation from long-term averages or the differences in rainfall between years. The third one is intra-annual rainfall variability, which is the distribution of rainfall within a year (Obasi, 2003).

In Ethiopia, literatures indicate that the distribution of rainfall and its variability has shown different phenomenon. According to National Meteorological Agency (NMA), 2007 the mean annual rainfall distribution over Ethiopia is characterized by large spatial variation which ranges from about 2000 mm over some highland areas in the Southwest to less than 250 mm over the Afar and Ogaden low lands. The basic climatic elements, in particular, rainfall shows seasonal or annual fluctuations somewhat different from normal expected climatic conditions in the country, which are very important to agriculture productivity (Shiferaw, 2014).

In Ethiopia, the climate variability impact that was somehow common to semi-arid region is also expanding to the highlands as highland environment is intervened by human intervention and global change (Getinet, 2010). Another study by Esubalew, (2014) revealed that long term recorded rainfall data showed an increasing trend between 1983 and 2012, with an overall mounting rate of 78.8 mm, except inter annual fluctuation and the mean maximum total rainfall analysis output of the same period lacks consistent pattern. Furthermore, late onset and early cessation of rainfall has also characterized in the escarpments of Arsi Mountains (one of Southeastern highlands) to central rift valley area. The study also revealed that, the climate variability is persistent particularly in the small rainy season ‘belg’, there was a decline in the amount of rainfall and affected vegetation condition and crop production.

Another report by the Inter-Governmental Panel on Climate Change (IPCC) (2014), annual rainfall, is likely to decrease throughout most of the African region, with the exception of

Eastern Africa, where annual rainfall is projected to increase. Trend analysis of annual rainfall in Ethiopia shows that rainfall remained more or less constant when averaged over the whole country while a declining trend has been observed over the Northern half of the country and Southwestern Ethiopia.

Moreover, various studies also revealed that there are different results in the seasonal and inter-annual trends of rainfall variability in the country as well as in different parts of the country. A review of studies in the works of Woldeamlake and Conwayb (2007), indicated that some studies have found no trends and others have found declining trends in terms of inter-annual and seasonal (in particular rainy seasons) in different parts of the country. They also stated that, "the main reason for the contrasting results of trend identification in annual rainfall in the central and northern highlands is the use of different periods in the analyses. In the region ("northern highlands") the 1980s were generally dry relative to preceding decades whilst rainfall recovered during the 1990s – trend analysis that ends during the late 1980s or early 1990s, therefore, shows a declining trend, however, when the period is extended this trend in annual rainfall is reduced or even removed. Seasonal and intra-seasonal trends may exist, as may more localized trends" (Woldeamlake and Conwayb, 2007: p. 1468).

The results of Woldeamlake and Conwayb, (2007), support those of the previous studies in Ethiopia and their findings indicate that: (1) High levels of spatial variability exist at sub regional scales in Ethiopia that are unlikely to be fully explained by large-scale climate influences; (2) Choice of study period strongly influences the results of trend analysis in this region due to the effects of decadal variability (particularly because the 1980s was the driest decade and the 1990s the wettest decade on record); (3) Annual rainfall in the region recovered during the 1990s, although 2001–2003 were average or slightly lower; and (4) There are no consistent emergent patterns or trends in daily rainfall characteristics in the drought-prone areas of Amhara region (northern highlands) of Ethiopia (Woldeamlake and Conwayb, 2007).

A recent study by El Kenawy et al., (2016) in Ethiopia the regions that receive less than 400 mm of annual precipitation showed a declining trend, with the largest changes occurring over Afar region. Generally, the highly elevated regions over the central Ethiopian Highlands showed the weakest changes, compared to the lowlands.

In the escarpments of Arsi Mountains of central rift valley, the proportion of forest coverage is significantly decreasing from time to time. The forest coverage has been reduced to 12258.4 ha (7.5%) by 2013 from that of 1984 having a total forest coverage of 19140.4ha (11.7%) (Esubalew N., 2014).

2.2.Remote Sensing for Monitoring Vegetation and Rainfall

Remote sensing can be defined as “the art, science and technology of observing an object, scene or phenomenon by instrument-based techniques. It is "remote" because observation is done at a distance, through a sensor, without physical contact with the object of interest (Lillesand et al., 2004).

There are two types of remote sensing instruments. These are passive sensors and active sensors. The first type detects natural energy (radiation) that is emitted or reflected by the object or scene being observed. Reflected sunlight is the most common source of radiation measured by passive sensors. On the other hand, active sensors provide their own source of energy to illuminate the objects they observe. An active sensor emits radiation in the direction of the target to be investigated. The sensor then detects and measures the radiation that is reflected or backscattered from the target (Ibid). In this study passive sensors are used for this paper. In principle, passive remote sensing works as follows:

1. Energy comes to the earth and a part is reflected and detected by a sensor.
2. This detection is captured as data, which are sent to a receiving station.
3. Some pre-processing takes place in the receiving station and then the pre-processed data are handed over to the users.
4. The users analyze the data for their own application.

There are different methods and techniques to monitor rainfall like ground rain gauge and global circulation models; and vegetation condition from field survey and satellite remote sensing etc. However, satellite based remote sensing has enormous advantages over other methods; to monitor rainfall and natural and agricultural vegetation condition (Rembold et al., 2013; Atzerberger , 2013). Satellite derived measurements will not substitute the ground observation, but used in combination of other techniques to reduce ground based problems like; high cost, lack of timeliness, and low spatial coverage (Rembold et al., 2013).

Moreover, satellite remote sensing has been widely used in the earth observation for monitoring different earth resources like land management, vegetation, hydrological processes, atmospheric circulations etc. From the widely used application of remote sensing is monitoring of vegetation patterns and meteorological information (like precipitation and temperature). This is monitored by the information received from the spectral characteristics of vegetation canopy and estimation of rainfall, detailed explanation is given in the following sub-sections.

2.2.1. Satellite Remote Sensing for Monitoring Vegetation

Green plants have a unique spectral reflectance which is influenced by their structure and composition. The proportion of radiation absorbed and reflected in different parts of the spectrum depends on the state, structure and composition of the plant. Healthy canopies of vegetation have unique characteristics in the visible (0.4 μm – 0.7 μm) and near infrared (0.7 – 2.5 μm) portion of the electromagnetic spectrum. In the visible part of the spectrum particularly in the blue (0.45 μm) and red (0.6 μm) plant pigment i.e. chlorophyll absorb strongly for the purpose of photosynthesis. However, in the near infrared region of the magnetic spectrum, the internal part of the leaves scatters and strongly reflects this portion of the spectrum. It is this strong contrast, between the amount of reflected energy in the red and near infrared regions of the electromagnetic spectrum that has been the focus of a large variety of attempts to develop quantitative indices of vegetation condition using remotely sensed imagery (George and Hanuschak, 2010; Atzerberger, 2013).

Moreover, satellite derived measurements from vegetation canopy reflectance properties in the visible and infrared magnetic spectrum is known as vegetation index/VIs/ can provide information about the vegetation status. Vegetation indices are dimensionless, radiometric measures usually involving a ratio and /or linear combination of the red and near-infrared (NIR) portion of the spectrum (Huete et al., 1994).

Jackson and Huete (1991) classified VIs into two groups: slope-based and distance-based VIs. Furthermore, Thiam and Eastman (2016) classified into three groups by adding orthogonal transformation. Different vegetation indices for the three major groups are indicated in the following table 1; more details of these can be found in the manual of Thiam and Eastman, (2016). The first group of vegetation index, i.e. slope based vegetation indices, is the interest of

this paper. These types of vegetation indices are basedon simple arithmetic combinations that focus on the contrast between the spectral response patterns of vegetation in the red and near infrared portions of the electromagnetic spectrum.

Table 2.1: Major categories of vegetation indices and sub-categories of vegetation indices

No.	Major Category	Vegetation Index	Proposed by
1	Slope Based VI	The Ratio Vegetation Index (RATIO)	Rouse, et al., (1974)
		The Normalized Difference Vegetation Index (NDVI)	Rouse et al., (1974)
		The Transformed Vegetation Index (TVI)	Deering et al., (1975)
		The Corrected Transformed Vegetation Index (CTVI)	Perry and Lautenschlager, (1984)
		Ratio Vegetation Index (RVI)	Richardson and Wiegand (1977)
		The Enhanced Vegetation Index (EVI)	In the works of Huete et. al., 2002
2	Distance Based VI	The Perpendicular Vegetation Index (PVI)	Richardson and Wiegand (1977)
		Difference Vegetation Index (DVI)	Richardson and Wiegand (1977)
		The Ashburn Vegetation Index (AVI)	Ashburn, 1978
		The Soil-Adjusted Vegetation Index (SAVI)	Huete (1988)
		The Transformed Soil-Adjusted Vegetation Index (TSAVI1)	Baret, et al. (1989)
		The Modified Soil-Adjusted Vegetation Indices (MSAVI1 and MSAVI2)	Qi, et al. (1994)
		The Weighted Difference Vegetation Index (WDVI)	attributed to Richardson and Wiegand (1977), and Clevers (1978) by Kerr and Pichon (1996)
3	Orthogonal Transformation	Principal Components Analysis (PCA)	Singh and Harrison, 1985; Fung and LeDrew, 1987; Thiam, 1997
		Misra's Green Vegetation Index (MGVI)	Wheeler et al. (1976) and Misra, et al. (1977)

Source: Thiam and Eastman, (2016).

From the different slope based VIs, Normalized Difference Vegetation Index (NDVI) by Rouse et al., in 1974 (Deering, 1978), used most often to study vegetation greenness, stress, health and crop production (Vrieling et al., 2011; Tucker et al., 1980; Sellers, 1985).It is expressed as the

difference between the near infrared and red bands normalized by the sum of those bands (Rouse et al., 1974; Gutman and Ignatov, 1998), i.e.:

$$\text{NDVI} = \frac{NIR - RED}{NIR + RED}$$

Where, NDVI is Normalized Difference Vegetation Index; NIR is near infra red; and RED is the visible spectrum of red.

NDVI is the most commonly used VI as it retains the ability to minimize topographic effects while producing a linear measurement scale. In addition, divisions by zero errors are significantly reduced. Furthermore, the measurement scale has the desirable property of ranging from -1 to 1 with 0 representing the approximate value of no vegetation. Thus negative values represent non-vegetated surfaces.

There are numerous satellites that are commonly used for monitoring vegetation dynamics by applying vegetation indices. From the different available satellites; low and medium spatial resolution satellites with high temporal resolution (high revisit time of the earth) offers better information for timely monitoring vegetation at global and regional scales. Among the low and medium resolution vegetation satellites, National Oceanic and Atmospheric Administration Advanced Very High Radiometric Resolution- Normalized Difference Vegetation Index (NOAA-AVHRR NDVI), VEGETATION SPOT, MODIS (Terra and Aqua), MERIS, ENVISAT and SENTINEL-2 are most widely used for monitoring vegetation.

NOAA-AVHRR was launched in 1981 and with its continuous series, is providing continuous data up to present time. The second vegetation satellite was launched in 1998 that the French-Belgian-Swedish satellite SPOT is equipped with a 1km resolution sensor for vegetation monitoring at global scale called VEGETATION. SPOT-VEGETATION was operational until 2014. In addition, starting from the end of the 20st century and the beginning of 21st century different satellites with better technologies have been launched. These includes; MODIS-Terra, which was launched on December 1999 for land observation and MODIS-Aqua was launched on 2002 and studies the precipitation, evaporation, and cycling of water. Envisat ("Environmental Satellite") was a large multi-sensor Earth-observing satellite which was launched on 2002 and

was operational until May 2012 (Rembold et al., 2013). The following section deals with the AVHRR NDVI satellite and its characteristics.

2.2.2. NOAA-AVHRR NDVI

It is only with the growing availability of low resolution multi-spectral satellite images from the meteorological satellite series NOAA AVHRR in the early 80's, that similar analyses are extended to large areas, including many countries in arid and semiarid climates. AVHRR (Advanced Very High Resolution Radiometer) is a broad-band scanner, sensing in the visible, near-infrared, and thermal infrared portions of the electromagnetic spectrum (Pinzon and Tucker, 2014).

Furthermore, data are obtained from two AVHRR instruments, the AVHRR/2 that flew from July 1981 to November 2000 and the AVHRR/3 instrument that is flying/has flown since November 2000 to present. These instruments have flown or are flying on fourteen National Oceanic and Atmospheric Administration (NOAA) polar-orbiting platforms in the TIROS-N/NOAA (A-D) series and in the Advanced TIROS-N (ATN)/NOAA (E-N') series (The National Oceanic and Atmospheric Administration (NOAA) and the National Aeronautics and Space Administration (NASA) have jointly developed this valuable series of polar-orbiting Operational Environmental Satellites (POES). NASA's Goddard Space Flight Center has managed the development and launch of the mission that encompasses the NOAA (A-N Prime) series of platforms (Pinzon and Tucker, 2014: p.6930). After NASA transferred operational control to NOAA, the name of the satellite changed from NOAA (A-N Prime) to NOAA.

Although AVHRR sensors were not originally intended as a climate mission (Cracknell, 2001), their early success for vegetation studies was due to a reconfiguration of the instruments to have non-overlapping ("visible") channel one (0.58–0.68 μm) and (near-infrared) channel two (0.725–1.10 μm) spectral bands (Tucker et al., 1975; Tucker and Maxwell, 1976). The reconfiguration enables the calculation of spectral vegetation indices such as the NDVI3g which is derived from channel 1 (0.63*m*m) and channel 2 (0.85 *m*m) and calculated as: (channel 2 − channel 1)/ (channel 2 + channel 1) (Tucker, 1979). The long record of AVHRR NDVI data has become particularly relevant for continued long-term monitoring of land surface.

Table 2.2: General characteristics of NOAA-AVHRR spectral vegetation index instruments and period of operation.

AVHRR Instrument	Instrument Series	Date of Operation	References, Comments
NOAA AVHRR/2	NOAA-7 (C)	July 1981 – February 1985	Deactivated June 1986
	NOAA-9 (F)	February 1985-September 1988	Deactivated February 1998
	NOAA-11 (H)	September 1988- September 1994	No data after September 1994
	NOAA-9 (F)-d	September 1994 – January 1995	Descending node, 9 am
	NOAA-14 (J)	January 1995 – November 2000	Late overpass after January 2001
NOAA AVHRR/3	NOAA-16 (L)	November 2000-December 2003	Data failure after January 2004
	NOAA-17 (M)	December 2003 – January 2009	No data after April 2010
	NOAA-18 (N)	08/2005 – Present	Data used after December 2007
	NOAA-19 (N')	06/2009 – Present	Data used after December 2011
	MetOp-A	10/2006 – Present	
	MetOp-B	September 2012 - Present	
	MetOp-C	2018 launch	

Source: Pinzon and Tucker, (2014:p.6932)

2.3.Satellite Remote Sensing for Monitoring Rainfall

Africa has a limited network of rain gauge stations and for various reasons a large number of existing rainfall records is incomplete. In addition to the poor availability of rainfall records, there is a steady decline of the standard observation network, which is a strong limitation for climate related research. Because of the presented limitations in the availability and quality of measured data, so called rainfall estimates have been developed. Rainfall estimates provide a spatial and temporal overview of the amount of rainfall based on a variety of input data (Meidment et al., 2014).

In the absence of long-term ground observations of rainfall across Africa, satellite-based rainfall estimates have provided a practical and complementary alternative. There are different rainfall estimation data sets available for Africa. Among others the widely used are the followings (FAO, 2014):

- The rainfall forecasts of the European Centre for Medium-Range Weather Forecast (ECMWF);
- The rainfall estimates (RFE) produced by the Climate Prediction Centre (CPC) of the NOAA;
- Tropical Rainfall Measuring Mission (TRMM): is a joint space mission between NASA and the Japan Aerospace Exploration Agency (JAXA) designed to monitor and study tropical rainfall. It is used for 35 degrees north and south latitudes.
- Tropical Applications of Meteorology using SATellite and ground-based observations (TAMSAT): is a research group at the University of Reading (UK). The products of the group are a 10-daily (dekadal), monthly and seasonal rainfall estimates for Africa derived from Meteosat thermal infra-red (TIR) channels based on the recognition of convective storm clouds and calibration against ground-based rain gauge data.

In tropical Africa, rain is mostly created by convective storms and the clouds with the coldest top surface produce the heaviest rainfall. It is possible to derive estimates of rainfall by measuring the cloud top temperatures (typically by satellite), and the length of time a cloud is at a critical threshold temperature. This methodology is known as the Cold Cloud Duration (CCD) (Milford, (n.d.)).

The basic methodology of the cold cloud statistics procedures is as follows. A regular series of thermal infrared (TIR) images of an area is received, pixels with apparent temperatures lower than some predetermined threshold are classified as "Cold Cloud", and their characteristics accumulated over some period. The resultant map is converted to a rainfall estimate, possibly with the help of information from other sources (which may be other satellite sensors or observations from the Earth's surface) (Milford, (n.d.: p.13).

The TAMSAT rainfall estimates are also based on the cold cloud duration model, but differently from the RFE algorithm, historical rainfall data are used for calibration which is done at the level of geographical calibration windows. The advantage of TAMSAT data is the higher availability of historical rainfall estimates as compared to near real time GTS station data. On the other hand, the disadvantage is that the fixed calibration windows sometimes lead to transition problems between windows.

The TAMSAT rainfall estimates and derived products are based on Meteosat thermal infra-red (TIR) imagery provided by EUMETSAT. The TIR is calibrated against an extensive ground-based rain gauge data archive. The last calibration was carried out in 2011 (Tarnavesky et al., 2014). The TAMSAT method combines geostationary Meteosat data with gauge observations through a calibration approach that exploits both data sources. The data are available as 10-daily data for Africa since 1981 to present and the operational production of the data at continental level has been supported by the European Commission of the Joint Research Centre.

There are three aspects to the TAMSAT system (Tarnavsky et al., 2014). The first is the calibration of the algorithm, using a newly compiled archive of rain gauge observations and contemporaneous cold cloud duration (CCD) fields. The calibration is carried out for 1983–2010. The second aspect is the provision of near-real-time rainfall estimates, derived by applying the calibration to the CCD generated from Meteosat imagery transmitted in real time. Finally, outside the calibration period (i.e., from 2011 onward), gauge data are used to independently validate dekadal TAMSAT rainfall estimates.

TAMSAT rainfall estimates have been available since the early 1990s and have been validated for several regions and applications. As indicated in Tarnavsky et al., (2014), comparisons with other available products have been carried out, including for Ethiopia (Dinku et al. 2007;

Dinkuet al. 2014), Kenya (Herman et al. 1997; Tucker and Sear 2001), West Africa (Laurent et al. 1998; Jobard et al. 2011; Snijders 1991), southern Africa (Thorne et al. 2001), and Uganda (Asadullah et al.2008; Maidment etal.2013).These results showed that the TAMSAT approach outperforms or is comparable to other available satellite-based datasets with similar spatial and temporal resolution and extent (Tarnavsky et al., 2014). On the other hand, some studies have been also conducted the reason for the accuracy of TAMSAT RFE and demonstrated the utility of the data as a complementary approach for estimating rainfall in gauge-sparse regions. These studies have been conducted on the earlier version of TAMSAT data which was calibrated for rain gauge data.

Moreover, validation of the TAMSAT data by Tarnavsky et al., (2014), have been extended to provide spatially contiguous rainfall estimates across Africa through new climatology-based calibration based on space and time.

2.4. NDVI in Response to Rainfall Variability

Different studies have been conducted on the relationship between vegetation-rainfall and the response of vegetation to rainfall variability by using NDVI and RFE. The existing studies have been conducted with different objectives. Among others rainfall variability and its impact on NDVI (Shisanya et al., 2011); Miguel et al., (2013) on the combined spatial and temporal effects of precipitation controls on long-term monthly NDVI in the Southern Africa Savanna; the precipitation–NDVI relationships in eastern and southern African savannas (Chamaillé& Fritz, 2009); Sahelian vegetation dynamics using NOAA-AVHRR NDVI data from 1981–2003 (Anyamba& Tucker, 2005). Similarly, studies revealed that strong relationship between natural vegetation and climatic elements has been described in wide range of research (Anyamba and Tucker, 2005; Fabricante et al., 2009).

According to United Nations Framework Convention on Climate Change (UNFCC), (2010), the vegetation coverage becomes sparse in many parts of the world and it is likely to become very sparse in places where the climate is highly variable. Moreover, there is a growing concern that the interaction between climate variability and vegetation dynamics; and existing investigations indicate that, the interaction between climatic factors and vegetation differs from one geographical region to another, where there are different unique climatic characteristics

influenced by various factors. The previous studies indicate that, major climatic elements, in particular rainfall and temperature, and NDVI have a positive relation in some region (Yang et al., 2011; Chammaile-Jammes and Fritz 2009; Nicholson et al., 1990). However, Zhong et al., (2010), indicated that, there is negative relationship in different regions depending on geographical position, geomorphology, vegetation type, climatic condition.

The findings of numerous studies revealed that, various results on the vegetation dynamics with respect to rainfall variability in different parts of Africa as well as in Ethiopia. A study by Rousvel et al., (2013) the annual cycles of both variables revealed a coherent onset, peak and decay, with a time lag of 1 month for almost all central Africa, except the areas, semi-desert and steppe, where a season of short and intense rainfall was observed. The correlation coefficients between the two variables are relatively high, especially in brush-grass savannah, where they reach up to 0.90 at a time lag of 1 month. The phenological transition points and phases show that the range between the +1 and −1 time lags corresponds to the duration of the maturity of vegetation. Overall, there is a strong similarity between temporal patterns of NDVI and rainfall.

A study by Getahun and Shefine, (2015) indicates that, climate variability is common and continuous to affect vegetation condition, particularly, in small rainy season in Gojjam Amhara region (in Northern central highlands) of Ethiopia. There is also a strong positive correlation between NDVI and the seasonal rainfall in most years. The NDVI anomaly pattern is almost similar to that of the main documented precipitation and temperature anomaly pattern associated with ENSO. The spatial and temporal analyses of basic climate elements and NDVI values for the growing season showed that NDVI and rainfall are highly variable during the 9 years period.

Another research indicates that, there is moderate positive correlation between NDVI and mean annual rainfall in most cases and ‘meher’ season whereas a strong correlation found between rainfall and NDVI in ‘belg’ season in the escarpments of Arsi Mountains to central rift valley region of Ethiopia (Esubalew, 2014).

At country level, Getahun, (2012) has concluded that, the spatial pattern of NDVI and precipitation showed that vegetation responded directly to precipitation. The seasonal patterns also showed that there was between 0 to 3 months lag between precipitation and vegetation. However, it was not possible to draw conclusion regarding the annual trends of precipitation and

NDVI because of the nature of the NDVI data, which was produced using the 10 day maximum composite values (Getahun, 2012).

Mekonnen Daba,(2016) has conducted a study on temporal relationship between NDVI and rainfall in the Southern Part of Ethiopia. The result of the study indicates that, the temporal pattern of NDVI and rainfall revealed that vegetation responded directly to rainfall. The temporal patterns showed that there was between 0 to 1 months lag between rainfall and vegetation. The results also showed that, the annual and monthly variability of NDVI is depending on the vegetation status and crop performance; thus it can be used to monitor the vegetation cover over the southern part of Ethiopia. The vegetation cover is high during the rainy season than dry season. It is believed that the increased status of NDVI over rainy seasons is due to the increased in vegetation coverage and cropping season. On monthly basis, the relation between rainfall and NDVI is strong but. The correlation is not such strong, when the cumulative annual amounts of rainfall are involved.

Another study has been also conducted on the assessment of rainfall anomalies in the semi-arid regions of Ethiopia by Worku and Csaplovics, (2015). The findings of their study (Worku and Csaplovics) indicate that, the growing season NDVI values are highly correlated with the precipitations during the whole study period. A lag of up to 30 days observed in most parts of our study region in which the rainfall has effects on vegetation growth after 40 days. The lag-time effects vary with the distribution of land use types and seasons. A lower correlation was observed in the woodland regions where significant deforestation occurred due to expansion of croplands. The loss in vegetation contributed to the low biomass production attributable to extended loss in vegetation cover.

CHAPTER THREE

MATERIALS AND METHODS

3.1.Study Area

The absolute location of the Awash River Basin lies between $7^0$52’12’’N and $12^0$08’24’’N latitude, and $37^0$56’24’’E and $43^0$17’24’’E longitude. The Awash River originates from the high plateau to the West of Addis Ababa, at an altitude of about 3,000 m, flowing eastwards through the Becho Plains before entering the Koka Reservoir, a dual-purpose dam for flood control and hydropower generation. It then flows in a north easterly direction through the northern extension of Rift Valley to eventually discharge in to Lake Abe near the Djibouti boarder at an altitude of 250m. Lake Abbe has an average size of 34,000 ha open water, surrounded by 11,000 ha of salt flats. The area is shrinking during dry years. The water level can drop up to 5 meters. The maximum depth is 36 m. The total length of the Awash River is approximately 1,250 kilometers.

It is the fourth populous basin in Ethiopia and ranks the 3rd of all basins of Ethiopia in terms of population density and stands 4th and 7th in its area and volume of water respectively. The overall population in the Awash Basin is estimated to be 14.9 million from the CSA report of 2007 G.C. -more than 65% of this concentrated in the Upper Awash. The Awash Basin covers a total area of 116,000 km^2 and has annual flow of 4.9 billion m^3.

The climate of the Awash River Basin varies from humid subtropical over central Ethiopia to arid over the Afar lowlands.The plateau areas of the basin (>2,500m a.m.s.l.) receive rainfall 1,000 – 1,400 mm and less than 200mm per year respectively. . Rainfall distribution is generally bimodal in the Middle and Lower Awash and unimodal in the Upper Awash. The highland areas have with a short rainy season during March and April and the long rainy season from June to September. The mean annual rainfall of the basin varies from about 1,600 mm, in the highlands north east of Addis Ababa, to 160 mm, in the northern point of the basin**.** The mean annual rainfall over the entire Western catchment is 850 mm and over the headwaters of the Awash, it is 1,216 mm. Over the Eastern catchment the mean annual rainfall is estimated to be 465 mm. Minor rains normally occur in March and April and major rains from July to August. As such, the occurrence of rainfall is highly erratic. The total amount of rainfall also varies greatly from year to year, resulting in severe droughts in some years and flooding in others (ABA, 2017). The

mean annual temperature ranges from 20.8^0 C to 29^0 C and the annual average wind speed is $1.2ms^{-1}$ (MoWE, 2011).

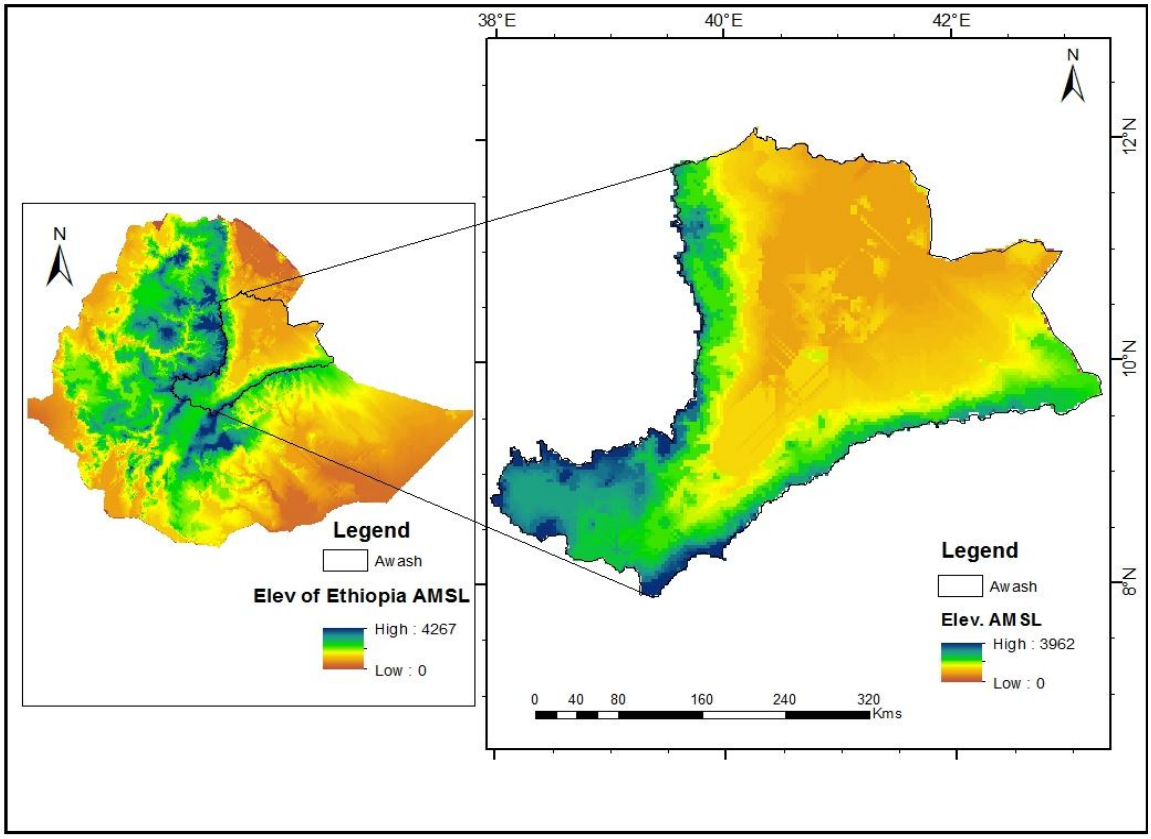

Figure 3.1: Map of the Study Area

The basin has two main physiographic components; the plateau land and Rift Valley, which covers most of the basin. The topography of the plateau is generally flat with elevations ranging from 2000 m to 3962m a.m.s.l.. The Rift Valley area is seismically active and there is a well-documented history of earthquakes and there are still places having active volcanic areas (MoWE, 2011; as cited in SifenAbera, 2012).

The soil types found in the study area are Pellic Vertisol, Vertic Cambisol, Chromic Luvisols, LuvicPhaeozems, and Lithosols. However, the dominant soil types are Cambisols and Vertisols. The vegetation cover in the upper and middle parts of the basin is grassland with some scrubland and riparian forest along the Awash River. Some of the plant species include Balanite saegypticus, Salix subserata, Flueggia Virosa, Carissa edulis, Rumexnervosus, Tamarin dusindica, Ulceaschimperi and Accacia species (Halcrow, 2006).

Awash River has major economic value for the country. There are various irrigation projects and sugarcane factories in the basin. The irrigation projects are 'Tendaho', 'Kesem', Awash Agro-Industry, etc; whereas the sugarcane plantation and factories include 'Matahara' and 'Wenji-shoa'. These plantations and factories have great economic development contribution for the country. Due to water availability and land resources, the Awash Basin is the most developed basin in Ethiopia.

3.2. Data Sources and Materials

3.2.1. GIMMS NDVI3g Data

NOAA- AVHRR NDVI3g (National Oceanic and Atmospheric Administration – Advanced Very High Resolution Radiometry; Normalized Difference Vegetation Index 3rd generation) data was obtained from Global Inventory Monitoring and Mapping Studies group (GIMMS NDVI3g) with spatial resolution of 0.08333^0 or 8 km and 15 days of Maximum Value Composite (MVC) image. The data was downloaded and processed for the period of 30 years from 1983 – 2012 from https://ecocast.arc.nasa.gov/data/pub/gimms/. The bi-weekly MVC NDVI3g data correction for aerosols, clouds, volcanic ash (for the periods between April 1982 and December 1984 and June 1991 and December 1993 (Vermote and Kaufman, 1995)) and sensor degradation has been done to improve the data quality by GIMMS research group (Kaufmann et al., 2000; Pinzon and Tucker, 2014). It is available freely from ECOCAST. For this study, a total of 720 NDVI3g images were used (2×12=24 image per year and 24×30=720 images for 30 years).

The raw GIMMS NDVI3g data has a value that ranges from -1000 to 1000 and this has been rescaled to -1 to 1. -1 is water bodies and 0 indicates that there is no vegetation. The spatial resolution was also resampled from 0.08333^0 /8km/ to 0.0375^0 /4km/ to fit with RFE resolution. This step was important for pixel wise comparison of the relationship between NDVI3g and RFE. Similarly, image masking was done by the study area. The GIMMS NDVI3g data was used in this study due to its long-term periodicity and free availability.

3.2.2. Rainfall Data

In this study monthly RFE Version 2 was obtained from Tropical Application of Meteorology using SATellite and Ground Rain gauge (TAMSAT) research group of University of Reading for the period from 1983 to 2012 (30 years). The TAMSAT data is calibrated with historical ground observations for rainfall estimation with spatial resolution of 0.0375^0 or 4km for African continent (Maidment et al., 2014 and Tarnavsky et al., 2014). The TAMSAT data has indicated better agreement with ground gauge measurement over Ethiopia (Tufa Dinku et al., 2007). TAMSAT rainfall estimates have been validated for several regions and applications. As indicated in Tarnavsky et al., (2014), comparisons with other available products have been carried out, including for Ethiopia (Dinku et al. 2007; Dinku et al. 2014), Kenya (Herman et al. 1997; Tucker and Sear 2001), West Africa (Snijders 1991; Laurent et al. 1998; Jobard et al. 2011), Southern Africa (Thorne et al. 2001), and Uganda (Asadullah et al.2008; Maidment etal.2013).These results showed that the TAMSAT approach outperforms or is comparable to other available satellite-based datasets with similar spatial and temporal resolution and extent (Tarnavsky et al., 2014). Data was obtained freely from www.tamsat.org.uk/public_data. The continental RFE V2 has been also masked for the study area i.e. Awash basin, Ethiopia.

3.2.3. Land Use Land Cover map

The LULC map of Awash Basin has been obtained from the collaboration work between the Ministry of Environment, Forestry and Climate Change and United Nations for Food and Agricultural Organization. This data was important for the analysis of the different type of the vegetation cover as well as to identify natural vegetation and agricultural vegetation (Rainfed and irrigation).

3.2.4. Software Used

Various software were used to analyze the spatial patterns of NDVI in response to rainfall variability from 1983 to 2012 in Awash basin Ethiopia. These include; IDRISI/Terrset Geospatial Monitoring and Modeling System from Clark labs, Clark University, ArcGIS 10.1 (Environmental System Research Institute (ESRI)), and ENVI 4.7 image processing software. The software used from Clark labs were IDRISI SILVA version 17.0, Terrset version 18.2 and version 18.3. The first one is an older version and was not compatible for the updated release of

GIMMS NDVI3g and in the second two versions; new update has been added for GIMMS NDVI3g image processing. The three software were used for three months in the actual demo i.e. each version of software have one month free trial. Image pre-processing activities have been processed by using IDRISI/Terrset software includes; image pre-processing (missing data interpolation, deseasoning, and detrending), inter-annual and seasonal trend analysis, and linear modeling to answer the main three research questions.

Similarly, ENVI 4.7 image processing software was used for image projection, rescaling, resampling and masking global NDVI3g and TAMSAT RFE in the Awash basin. Lastly, ArcGIS was used to produce the outputs of the image used includes; (1) zonal statistics as a table to produce statistical results for all major vegetation types; (2) cell statistics to produce the long term results of mean, minimum and maximum values of NDVI3g and RFE

3.3. Image Preprocessing

In addition to routine image preprocessing activities (downloading image, projecting, rescalling, resampling, and masking with the study area), other image preprocessing techniques have been also conducted. These includes, (1) missing data interpolation and image gap filling; avoiding the impact of seasonal variation for long term inter-annual analysis i.e. Deseasoning (2), first order serial correlation correction/Trend Preserving Prewhitening/(3).

The daily coverage of low and medium resolution NDVI images have different problems associated with; sensor related artifacts, atmospheric noise, water vapor, undetected clouds, soil background, and BDRF of sensor view angle; consequently affects the value of NDVI (Goward et al., 1991; Atzerberger and Eilers, 2011).Therefore, before conducting any spatio-temporal image time series analysis, different image processing should be conducted.

The daily NDVI3g image has been composited to Maximum Value Composite (15 day MVC) to compensate some artifacts present in the daily images. In this regard, Holben (1986) stated that, compositing daily images to Maximum Value Composite (MVC) NDVI image, will only reduce and eliminates noise from the image resulted from sensor related artifacts, (Atzerberger and Eilers, 2011), still requires further process. Equally important, temporal smoothing and filtering is also necessary to get smoothed NDVI. There are different filtering techniques for temporal smoothing and gap filling as well as continuous to grow (Hird and McDermid, 2009). Currently,

there is no commonly used and consensus on the smoothing techniques (Atzerberger and Eilers, 2011). An interesting review of different filtering techniques with their advantages and drawbacks has been summarized in the works of Atzerberger and Eilers (2011); Atzerberger, (2013); Atkinson et al. (2012); White et al. (2009).

In this study, Harmonic Interpolation has been carried out. It is closely based on the procedure known as HANTS (Harmonic Analysis of Time Series) by Roerink et al. (2000). The procedure is best for filling missing data in mid-latitude areas. This procedure also fills in missing or noisy pixel values by fitting a harmonic regression to a one year window centered on that time period and then using the predicted pixel value to replace the missing or incorrect pixels (Eastman, 2016). Detailed explanation and techniques used in the HANTS algorism as well as different procedures have been briefly described in the works of Roerink, et al. (2000) and Teferi et al. (2015). This procedure was used, first to produce gapless image. In this case, the monthly TAMSAT RFE V2 is available if the three decadal data are available within the month, otherwise there will be missing data. In other words, there are some data gaps in the monthly RFE V2 data particularly during the 1980s. Second, to filter noisy pixels of both NDVI3g and RFE that is introduced from cloud contamination and other artifacts. The filtered 15 days MVC NDVI3g have been aggregated by the mean of two monthly images of the whole series data to produce a total of 360 images (12 images per a year ×30 years =360).

In long term image time series analysis, seasonal variation/cycle like El-Niño Southern Oscillation (ENSO) would have an impact. In other words, satellite observation is prone to the effects of annual cycle or seasonality, for example, vegetation development, is influenced by this effect. Therefore, before analyzing the inter-annual trend analysis, seasonal cycle has been removed by a procedure called de-seasoning (Ermias et al., 2015). Standardized anomalies (Z-score) procedure has been performed for both monthly RFE and aggregated mean monthly NDVI3g.

Standardized anomalies calculate the deviation from the long-term mean. Then when the anomaly images are created (by subtracting the long term mean) the result is divided by the standard deviation to create a standardized anomaly (a z-score). In this system, a value of 0

would mean that it has a value equal to the long term mean; a value of +1 would mean that it is 1 standard deviation of the long term mean, and so on.

Finally, in time series analysis, particularly in trying to assess the relationship between two or more variables, it is essential to consider autocorrelation or serial correlation. It is defined as the correlation of a variable with itself over successive time intervals, prior to testing for trends. Autocorrelation increases the chances of detecting significant trends even if they are absent and vice versa. Trend Preserving Prewhitenning corrects serial correlation for those regions which show significant serial correlation at a 95% confidence level using the Durbin-Watson test (Cochrane and Orcutt, 1949). The Durbin-Watson option detects the first order autocorrelation present in the residuals from a regression analysis using the Durbin-Watson statistic. Therefore, trend preserving prewhitening has been used to eliminate the presence of first order serial correlation present in the monthly mean NDVI3g and monthly mean standardized anomaly NDVI3g time series as well as in the filtered monthly RFE time series data.

3.4. Methods of Data Analysis

Before conducting the relationship and the response of vegetation to rainfall variability, conducting trend analysis would help to better understand the relationship between vegetation in response to rainfall variability. Owing to this fact, two types of trend analysis have been conducted i.e. Inter-annual and seasonal trend analysis of NDVI and rainfall.

3.4.1. Inter-annual Trend Analysis

For the purpose of inter-annual trend analysis of NDVI3g and RFE; monotonic trend analysis and linear trend analysis (Median trend (Theil-Sen slope estimator)) as well as Mann-Kendal significance test for monotonic trend analysis have been employed on both images.

The first technique was nonparametric monotonic trend analysis. The monotonic trend analysis is calculated from Mann-Kendal statistical test that measures whether x values tend to consistently increasing or decreasing over time (Neeti and Eastman, 2011). According to Donald et al. (2011), the statistical trend analysis is a null hypothesis (H_0) testing process, which assumes

there is no trend. The null hypothesis is tested against the alternative hypothesis H_1, which assumes that there is a trend.

The Mann-Kendall test analyzes the sign of the difference between later-measured data and earlier-measured data. Each later-measured value is compared to all values measured earlier; resulting in a total of n (n-1)/2 possible pairs of data, where n is the total number of observations. The Mann-Kendall test assumes that a value can always be declared less than, greater than, or equal to another value (Donald et al. 2011; and Neeti and Eastman, 2011). To perform a Mann-Kendall test (Mann, 1945 and Kendal, 1975), compute the difference between the later-measured value and all earlier-measured values, (x_j-x_i), where j>i. The test statistics, S, is computed as:

$$S = \sum_{i=1}^{n-1} \sum_{j=i+1}^{n} sign\left(x_i - x_j\right)$$

and $$sign\left(x_i - x_j\right) = \begin{cases} 1 & if \quad x_i - x_j < 0 \\ 0 & if \quad x_i - x_j = 0 \\ -1 & if \quad x_i - x_j > 0 \end{cases}$$

where *n* is the length of the time series data set and x_i and x_j are the observations at times *i* and *j*, respectively. The result of S statistic has an integer value of 1, 0, or -1. When S is positive number, earlier measured values tend to be less than later values and an increasing trend is indicated. When S is negative number, later values tend to be smaller than earlier values and a downward trend is indicated (Donald el al. 2011). A value of 0 indicates no consistent trend. It is calculated in a similar fashion to the median trend. All pairwise combinations of values over time are evaluated at each pixel and a tally is made of the numbers that are increasing or are decreasing with time. The Mann-Kendall statistic is simply the relative frequency of increases minus the relative frequency of decreases (Neeti and Eastman, 2011).

Similarly, Mann-Kendal significance test was applied to test the significance of monotonic trend. According to Mann (1945) and Kendall (1975); as indicated in Neeti and Eastman, (2011) the statistic *S* is approximately normal when n≥8. When there is no tie between data values then the mean and variance is given by:

$$E(S) = 0$$

$$\text{Var}(S) = \frac{n(n-1)(2n+5)}{18} = \sigma^2$$

where (σ^2) is the standard deviation.

When there exist ties between the data values, then variance is computed as

$$\text{Var}(S) = \frac{n(n-1)(2n+5) - \sum_{i=1}^{n} t_i(i)(i-)(2i+5)}{18}$$

Where t_i denotes the number of ties of extent i. (i.e. a dataset with two tied values would have one tie of extent two or $i = 2$ and $t_2 = 1$) (Douglas et al. 2000). The standardized *Z* test statistic is computed by:

$$Z = \begin{cases} \frac{S-1}{\sqrt{Var(S)}} & for \quad S > 0 \\ 0 & for \quad S = 0 \\ \frac{S+1}{\sqrt{Var(S)}} & for \quad S < 0 \end{cases}$$

The Z statistic follows the standard normal distribution with zero mean and unit variance under the null hypothesis of no trend. A positive Z value indicates an upward trend whereas a negative value indicates a downward trend.

The Mann-Kendall Significance measure in z-scores allows both the significance and direction of the trend simultaneously. Trends with high numbers imply stronger evidence. Critical values are +/- 1.96 for 5% probability of chance. Z-score with greater than +1.96 the trend indicates significantly increasing trend, a value with less than -1.96 shows significantly decreasing trend, and Z-score value between +1.96 and -1.96 indicates no significant trend in the time series.

On the other hand, if there is a significant monotonic trend (increasing or decreasing), it is important to measure the degree of change. This is done by applying median trend analysis, Theil-Sen slope estimator. Median trend uses a robust non-parametric trend operator that is highly recommended for assessing the rate of change (Haoglin et al. 2000). Median trend calculates the non-parametric Theil-Sen slope and intercept of the series. It is calculated by determining the slope between every pair wise combination and then finding the median value. For example, with a 20 year sequence of monthly data, a total of 28,680 slopes would be evaluated at every pixel. An interesting feature of the median trend is its breakdown bound. The breakdown bound for a robust statistic is the number of wild values that can occur within a series before it will be affected. For the median trend, the breakdown bound is approximately 29%. Thus the trends expressed in the image have to have persisted for more than 29% of the length of the series (in time steps).

3.4.2. Seasonal Trend Analysis

The tong-term inter-annual trend analysis result indicates that, there is change in the environment. In other words, they don't indicate when in the year that change is occurring and areas that show no trend (such as in the average NDVI for an area) may in fact be undergoing a change in seasonality where the changes balance to yield the same average (Eastman et al., 2009). This will be solved by applying seasonal trend analysis.

In this study, the seasonal trend analysis (STA) approach developed by Eastman et al. (2009) has been used. The procedure is based on two stages; in the first stage, harmonic regression is applied (separately for each pixel over time) to each year of images in the time series. The seasonality for all pixels is expressed in the form of five harmonic shape parameter images for each year to extract: the mean annual image (Amplitude 0), the annual cycle or peak of the annual cycle (Amplitude 1 and Phase 1) and the semi-annual cycle (Amplitude 2 and Phase 2). The amplitude images have greatest information; and the semi-annual cycle is simply to modify the shape of the annual curve. Therefore, mean annual image (amplitude 0), and annual cycle (amplitude 1) have been applied to both NDVI3g and RFE image time series.

In the second stage, trends over years in these five harmonic series shape parameters are analyzed using a robust non-parametric linear trend procedure. In other words, the trends are calculated using the Theil-Sen median slope method, again analyzing each pixel separately over time. This procedure calculates the slope for each pair wise combination of samples in time. The median of these slopes is then used to characterize the trend, resulting over all pixels in a separate trend map for each of the five shape parameters (Hoaglin et al. 2000, Huth and Pokorna 2004; as cited in Eastman et.al. (2009)).

Similarly, the number of harmonics would be resulted by the number of cycles. It is recommended that, 2 harmonics is better as the higher number of the harmonics will be affected by noise. Therefore, in this study 2 harmonics and 5 parameters have been applied on both images to assess the seasonal trend analysis. Likewise, amplitude 0 (mean annual), amplitude 1 (annual cycle/or peak of the series), and observed seasonal curves (the mean value of each months of the first five years (1983 – 1987) and the last five years (2008 – 2012) of the time series have been used.

3.4.3. Linear Correlation between NDVI and Rainfall Variability

Linear correlation was employed by using linear modeling. This modeling was used to assess the relationship between vegetation and rainfall in the time series from 1983 to 2012. In this case, the dependent variable is vegetation and independent variable is rainfall variability. In doing so, this procedure also have an advantage to map areas with high relationship and low relationship. The series relationship has been analyzed by using different lags i.e. lag 0, lag 1 and lag 3. Moreover, lag 0, implies that the dependent and independent series variables are compared at similar time steps. This means, both variable will begin and end at similar time. Positive lag-called *lag* indicates that, the independent variable i.e. rainfall, shifts to an earlier time than vegetation growth and development; whereas, negative lag-called *lead* indicates that, vegetation growth and development shifts earlier time than rainfall. The time interval between rainfall event and the time when precipitated water might reach a plant root and affect plant growth can vary from 1 to 12 weeks depending on vegetation types (Li et al. 2002).

CHAPTER-FOUR

RESULTS AND DISCUSSION

4.1 Inter-annual Trend Analysis of NDVI and Rainfall

4.1.1 Inter-annual Trend of NDVI

One of the most important analyses of time series is in search of trends. As indicated in the methodology part, the presence of trends has been measured by using monotonic trend analysis which was computed by Mann-Kendal statistics (Mann-Kendal Tau). Similarly, the Mann-Kendal statistics have been also tested by using Mann-Kendal Significance test and the magnitude of change have been also computed by median trend analysis by using Theil-Sen slope operator. The following discussion focuses on the two main trend estimators i.e. Mann-Kendal significance test (Z-score) and Theil-Sen Slope.

The finding of the study indicates that, there is decreasing trends of long term mean NDVI value based on the Mann-Kendal statistic result. The following table 4.1 and Figure 4.1 shows Mann-Kendal significance of trend and magnitude of change (table 4.2 and Figure 4.1) in the Awash basin and different land cover classes. Awash basin has a decreasing trend with mean annual rate of change 0.0082 NDVI yr^{-1} (-0.00068 *12) (table 4.2). Except for the grasslands with a rate of change 0.0003948 NDVI yr^{-1}, all vegetation types have shown decreasing trend over the entire period from 1983 – 2012. In this regard different land cover classes have shown decreasing trend with annual rate of change which includes agricultural land with long term mean annual rate of negative 0.00216 NDVI yr^{-1}; shrubland with a mean rate of -0.00816 NDVI yr^{-1}; bareland with -0.01549 NDVI per year; dense woodland -0.00456 NDVI yr^{-1} ; and forest with a rate of change -0.00088 NDVI yr^{-1} (table 4.2).

Moreover, Awash basin has different level of significance with a statistical results of 34.29 % negatively significance, no significance 35.78 % and 29.92 % positively significance (table 4.1). Similarly, the major land cover classes also have different significance level. As indicated in table 4.1, the highest three decreasing (negatively) significance trend (browning) had been observed in the land covers of shrubland (45.86 %), dense woodland (31.25 %) and agricultural land (26.96 %). On the other hand, bareland with 55.88 %, forest with 33.68 % and 25. 9 % of

dense woodland had shown increasing (greening) or positively significance trends over the three decades from 1983 to 2012 (table 4.1).

Table 4.1: Mathematical results of the Mann-Kendal Significance of Z-score

Land Cover Types	Area in Km^2	Area coverage in %	Mann-Kendal significance			Z-score		
			MIN	MAX	MEAN	Negatively significance	No Significance	Positively significance
Agricultural Land	29899.56	25.69	-11.47	12.32	-0.34	26.96	50.1	22.94
Grassland	5242.03	0.45	-11.96	11.28	0.35	20.33	45.67	34
Shrubland	29840.56	25.64	-13.43	12.47	-1.43	45.86	31.46	22.68
Bareland	40967.53	35.20	-13.4487	13.08	-2.79645	5.89	38.23	55.88
Dense WL	4479.933	0.38	-11.88	10.52	-0.48994	31.25	42.85	25.9
Forest	3279.143	0.28	-11.83	11.72	0.589706	23.52	42.8	33.68
Awash basin	116382.9		-13.45	13.08	-1.46	34.295	35.782	29.923

Other land cover types have the remaining 12.36% from the total area of Awash basin.

Table 4.2: Inter-annual Theil-Sen slope of NDVI

Land Cover Classes	MIN	MAX	MEAN	Rate of change per year (Mean*12)
Agricultural Land	-0.00716	0.006983	-0.00018	-0.00216
Grassland	-0.0062	0.006025	0.000329	0.003948
Shrubland	-0.00684	0.006956	-0.00068	-0.00816
Bareland	-0.00698	0.007118	-0.001291	-0.01549
Dense woodland	-0.00607	0.005067	-0.00038	-0.00456
Forest	-0.0069	0.0061	-0.000073	-0.00088
Awash Bsain	-0.007156	0.007118	-0.00068	-0.00816

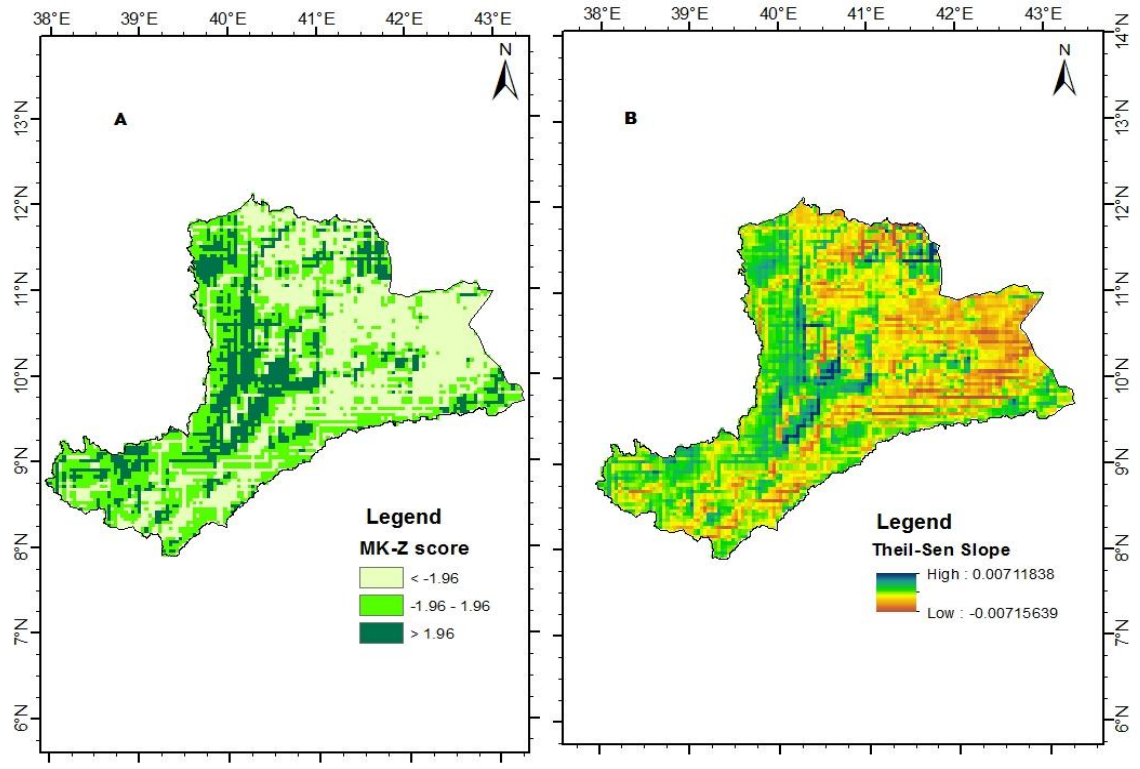

Figure 4.1: Inter-annual NDVI MK Z-score (A), Theil-Sen Slope (B) and LCLU Awash basin (C)

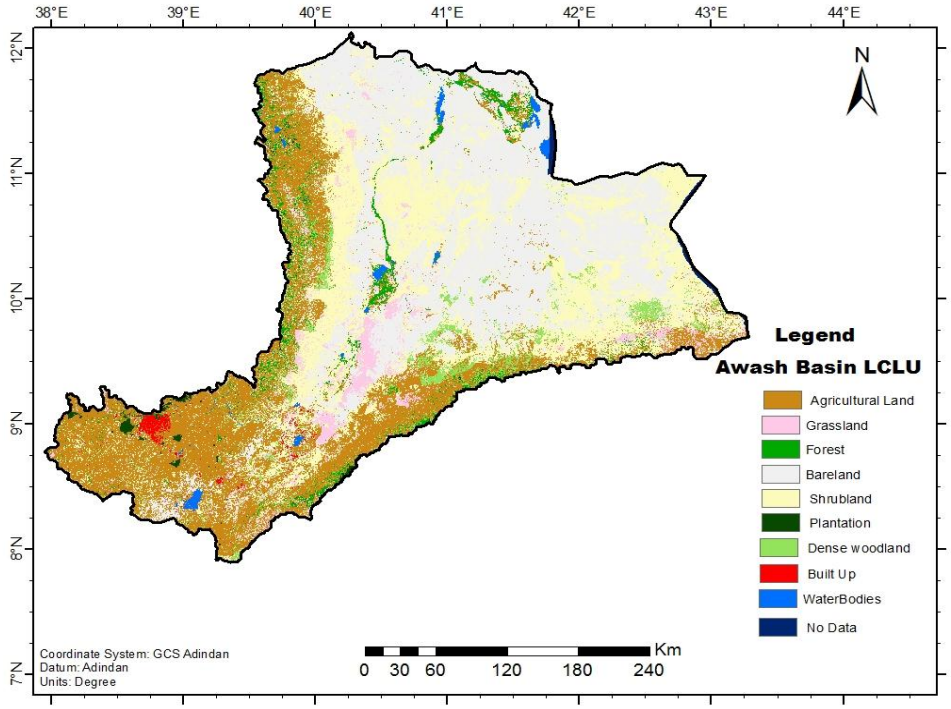

4.1.2. Inter-Annual Trends of Rainfall

Apart from the overall decreasing trend of vegetation with negatively, positively and no significance level; rainfall had shown an increasing trend from the mean Mann-Kendal significance result. Moreover, the trends have no significance and positively significance in the Awash basin for 30 years from 1983 – 2012 (table 4.3).

Table 4.3 depicts the inter-annual rainfall trends in the Awash basin from 1983 to 2012. It can be observed from the long term mean monthly rainfall revealed an increasing trend in Awash basin; however, the increments in the majority parts of the basin have no significance (65.13 %) and 34.87 % have increasing significantly with the rate of change 0.006468 mm per year (table 4.3). In the same vein, different land cover classes have also observed different level of significance and magnitude of change. From the table 4.3, it can be concluded that, the highest percentage (60.07 %) of grassland have positively significant (with the rate of change of 0.008796 mm per year); followed by agricultural land positively significance in 49.74% from the total land cover with a rate of change 0.008616 mm per year. Similarly, dense woodland areas have 47.58 % positively significant with a rate of 0.008616 mm per year, shrubland (32.74 %) and forest classes (29.95 %) with a rate of 0.005388 mm per year and 0.0057 mm per year.

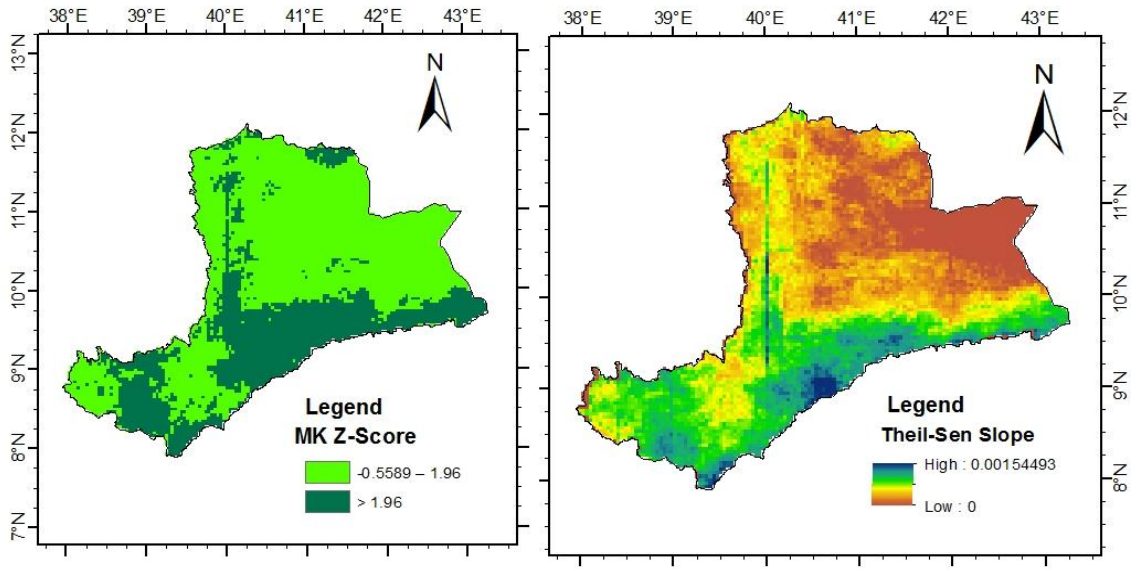

Figure 4.2: Inter-annual RFE MK Z-score and Theil-Sen Slope

Table 4.3: Mann-Kendal Significance of Z-score and Theil-Sen slope for rainfall

Mann-Kendal Z-Score					
Land Cover Type	MIN	MAX	MEAN	No Sign.	+vely Sign.
Agricultural Land	-0.39324	4.199231	1.993432	50.26	49.74
Grassland	0	3.724873	2.203121	39.93	60.07
Shrubland	-0.50675	3.817897	1.632649	67.26	32.74
Bareland	-0.55892	4.11553	1.378499	78.45	21.55
Dense woodland	-0.07496	3.429955	2.11318	52.42	47.58
Forest	0	3.382522	1.715038	70.05	29.95
Awash Basin	-0.558918	4.199231	1.66791	65.13	34.87
Theil-Sen Slope					
	MIN	MAX	MEAN	Rate of change per year	
Agricultural Land	0	0.001545	0.000734	0.008808	
Grassland	0	0.001543	0.000733	0.008796	
Shrubland	0	0.001372	0.000449	0.005388	
Bareland	0	0.001292	0.00031	0.00372	
Dense woodland	0	0.001434	0.000718	0.008616	
Forest	0	0.001435	0.000475	0.0057	
Awash Basin	0.0000514	0.001224	0.000539	0.006468	

4.2. Seasonal Trend Analysis of NDVI and Rainfall

The above results of inter-annual trends for NDVI and rainfall shows the trend over the entire time series years i.e. from 1983 to 2012. However, it is difficult to answer questionslike, when did the change has occurred within a year or between years? In which months the change has occurred? and so on. In other words, seasonal trend analysis will solve this problem. This is evident that, the annual cycle of solar energy input, different environmental phenomenon reveals seasonal cycle including rainfall and vegetation phenology. This study has been also undertaken for seasonal trend analysis in Awash basin. As explained in the methodology part, amplitude images have greater information as well as the semi-annual cycle (amplitude 2 and phase 2) are simply shape parameters of the annual cycle. Therefore, the following discussion focuses on amplitude 0, amplitude 1, and observed curve from 1983 to 2012.

4.2.1. Seasonal Trend Analysis of NDVI

Amplitude 0 is the mean annual value of vegetation greenness or browning. As indicated in table 4.5, the mean of CMK indicates there is a decreasing trend in Awash basin; however, from the total area of the basin about 42.56 % has shown seasonal trend. From this result, about 31.8% has observed a decreasing (browning) trend and only about 10.76 % has observed an increasing trend. More than half parts of the basin had observed trends but with no significance (57.44 %) (table 4.5). On the other hand, significantly decreasing trends have been observed in the major land cover types, for e.g., barelands about 48.5 % with a rate of -0.01068 NDVI per year , shrubland about 34.28% with a rate of change -0.00456 NDVI per year and agricultural land (13.81 %) at a rate of change -0.0024 NDVI per year. However, increasing trends of the mean annual seasonal trend have been observed in grassland (24.1 %) with a rate of 0.004956 NDVI per year, forest (18.78 %) with a rate of 0.003204 NDVI per a year (table 4.6).

Table 4.5: NDVI amplitude 0 of CMK-statistics and level of significance

Land Cover Type	Mann-Kendal Statistics			Level of Significance		
	MIN	MAX	MEAN	Negatively Significance	No Significance	Positive Significance
Agricultural Land	-4.23335	4.471059	-0.2372	13.81	78.36	7.83
Grassland	-3.61126	4.608712	0.24082	10.89	65.01	24.1
Shrubland	-4.67614	4.588717	-0.67556	34.28	50.35	15.37
Bareland	-4.43245	4.48216	-1.4606	48.5	44.88	6.62
Dense woodland	-3.99928	3.499864	-0.44923	22.9	70.94	6.16
Forest	-3.69275	4.456251	0.329056	14.22	67	18.78
Awash Basin	-3.75854	3.979522	-0.13753	31.8	57.44	10.76

Table 4.6 Amplitude 0 Median trend of Theil-Sen slope

Land Cover Type	MIN	Max	Mean	Rate of change yr^{-1}
Agricultural Land	-0.0104	0.009967	-0.0002	-0.0024
Grassland	-0.00732	0.009491	0.000413	0.004956
Shrubland	-0.012	0.013781	-0.00038	-0.00456
Bareland	-0.01368	0.01167	-0.00089	-0.01068
Dense woodland	-0.00828	0.005397	-0.0004	-0.0048
Forest	-0.01593	0.012588	0.000267	0.003204
Awash Basin	-0.00876	0.008653	-0.00012	-0.00144

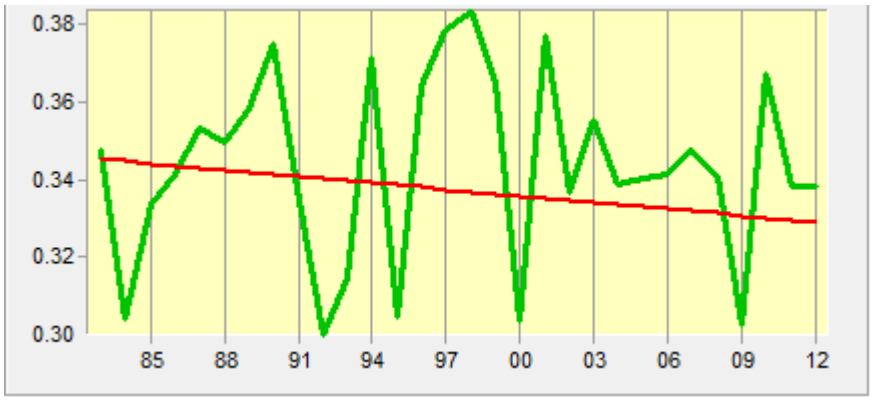

Figure 4.3: Seasonal trends of NDVI amplitude 0 (x-axis is year from 1983 – 2012 and y-axis is NDVI value)

As it is observed in the above figure 4.3, amplitude 0 of the Awash basin indicates that, there had been generally decreasing trend of mean annual vegetation greenness with irregular patterns. It is evident from the above figure some seasons had highest; while others had the lowest NDVI value. The lowest NDVI have been recorded in the years of 1983-1984, 1992-1993, 1995-1996, 2000 and 2008/2009; whereas the highest peaks of NDVI value throughout 30 years (1983 - 2012) were recorded in1990, 1994, 1997 – 1998, 2001 – 2002 and 2010 – 2011. In other words, the lowest NDVI value indicate the driest season while the highest peaks of NDVI indicates the wettest seasons throughout the studied period from 1983 – 2012 in the Awash basin.

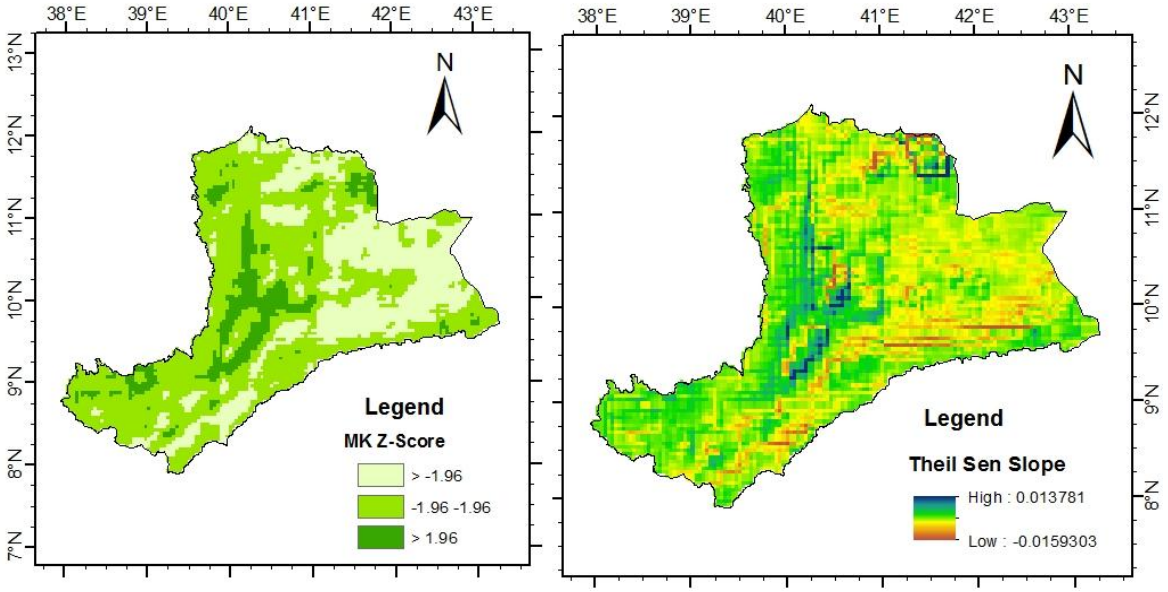

Figure 4.4: Seasonal trend of NDVI amplitude 0

Table 4.7: Amplitude 1 of Seasonal NDVI

Land Cover Type	Mann-Kendal Significance			Level of Significance		
	MIN	MAX	MEAN	Negatively significance	No Significance	Positively Significance
Agricultural	-2.59708	4.314578	2.084537	0.35	40.95	58.7
Grassland	-1.9079	3.998942	1.809837	0.33	53.14	46.53
Shrubland	-3.52954	4.191302	1.023657	1.12	68.51	30.37
Bareland	-3.18818	3.970277	0.544249	1.22	86.25	12.53
Dense WL	-2.72683	4.134912	1.535956	2.2	57.71	40.09
Forest	-2.1229	3.605836	1.511922	0.51	54.82	44.67
Awash Basin	-2.02304	3.674373	1.256428	0.573	69.004	30.423

The other result was obtained from Amplitude 1, which shows the peak of annual greenness. Table 4.7 indicates that, in the Awash basin the annual greenness had been increasing, but more than half of the basin areas (69%) had shown an increasing trend with no significance level. Table 4.7 also reveals that, the major land cover types had also shown increasing trend in the annual greenness with high positively significance (greenness) in agricultural land (58.7%), grass

land (46.53 %), forest (44.67 %) and dense woodland (40.09 %). Moreover, except for agricultural land, all land covers had shown more than half of the areas have no significance in the annual greenness. This is evident that, agricultural (crop) land has high seasonality followed by the rainy season of the year.

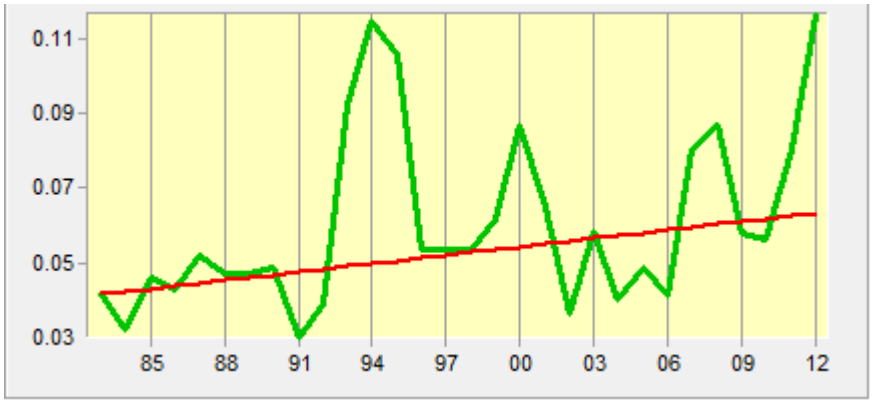

Figure 4.5: Amplitude 1 of NDVI (x-axis is year from 1983 – 2012 and y-axis is NDVI value)

On the other hand, as indicated in the above figure 4.5 for the total Awash basin, the year 1994 had revealed as the maximum peak of NDVI value from all 30 years (1983 – 2012) and followed by the year 2012 in the Awash basin. These two highest peaks represent as wettest years.

The other result of the study was also obtained from the observed seasonal curve (Figure 4.6). It is the median value for individual months over the first 5 years (1983-1987 in green color) and the last 5 years (2008 – 2012 in red color) in Figure 4.6. This is a type of short time series which can be affected by noise. Though, they can provide information about the modeled fitted curve.

Figure 4.6 indicates that, the results of the observed curve of the maximum values i.e. 0.37 for the first five years (1983-1987) is observed in 3rd week of August and browning started in 4th week of September; whereas for the last five years (2008 – 2012) vegetation green up with NDVI value of 0.40 starts in the 1st week of August and browning begins in the 3rd week of September. This indicates that, the vegetation green up for the last five years (2008 – 2012) starts two weeks earlier than the first five years (1983 – 1987). However, vegetation browning starts one week earlier in the last five years than the first five years. The last five years have also better NDVI values than the first five years during the major rainy season (Fig. 4.6). This indicates that

the rainy seasons for the last five years (2008 – 2012) have better influence on the vegetation growth and development in the Awash basin.

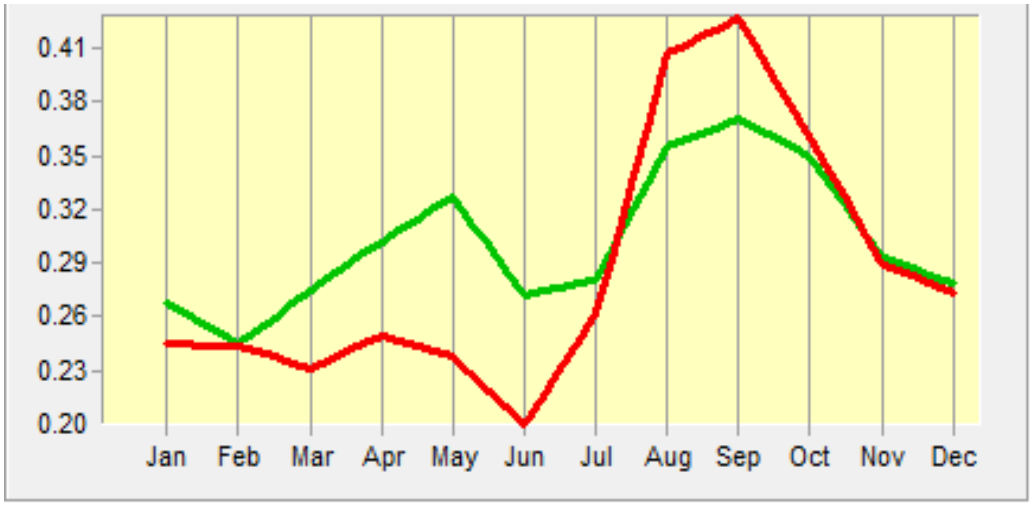

Figure 4.5: Observed seasonal curve of NDVI for the first 5 years (1983-1987 in green color) and the last 5 years (2008 – 2012 in red color).

4.2.2. Seasonal Trend Analysis of Rainfall

The mean annual rainfall (amplitude 0) and annual peak of rainfall (amplitude 1) had observed increasing trend over the entire studied period of the three decades from 1983 to 2012 in the Awash basin (table 4.8 and table 4.9). As depicted in table 4.8 and figure 4.6 (A-dark blue color), a significant increase in mean annual rainfall has shown in 43.54 % from the entire catchment area of Awash basin and 56.46 % of the catchment has no significance. Moreover, an increasing trend in mean annual rainfall trend had been also observed over different land cover classes in Awash basin (table 4.8). As revealed in table 4.8, the highest positive significant trends were observed in dense woodland (59.47 % of the area) with a mean rate of change 3.403812 mm per year; shrubland (45.79%) and grassland (45.54 %). However, the high rate of change in increments has been observed over agricultural land with a mean rate of 3.674964 mm per year (table 4.8).

Table 4.8: Summaries of amplitude 0 for CMK Z-score and Theil-Sen Slope

CMK Z-Score					
Land Cover Type	MIN	MAX	MEAN	No Signi.	+ velySigni.
Agricultural	0	3.321424	1.85982	58.22	41.78
Grassland	0	3.196446	1.98262	54.46	45.54
Shrubland	0	3.332678	1.913101	54.21	45.79
Bareland	0	3.381616	1.849463	58.41	41.59
Dense woodland	0	3.128947	1.929353	40.53	59.47
Forest	0	3.290988	1.889403	53.3	46.7
Awash Basin	0	3.381616	1.876542	56.46	43.54
Theil-Sen Slope					
Land Cover Type	MIN	MAX	MEAN	Rate of change year^{-1}	
Agricultural Land	0	0.702637	0.306247	3.674964	
Grassland	0	0.625679	0.28758	3.45096	
Shrubland	0	0.668142	0.253768	3.045216	
Bareland	-0.09375	0.561515	0.202016	2.424192	
Dense woodland	0	0.565123	0.283651	3.403812	
Forest	0	0.660922	0.251939	3.023268	
Awash Basin	0.029716	0.550978	0.26169	3.140279	

It can be observed from Fig. 4.7 (bottom) that, in the first five years from 1983-1987 (green color), rainfall record has been observed in the second week of June which is one month later than the last five years (2008-2012) i.e. second week of May. Similarly, the end of rainfall record has been observed for the first five years was in the beginning of September and for the last five years it was during the end of August. Generally the rainfall in the study area, showed an increasing trends both in terms of seasonal length and start of the season.

Table 4.9: Amplitude 1 CMK of RFE

1. CMK Z-Score					
Land Cover Type	**MIN**	**MAX**	**MEAN**	**No Signi.**	**+velySigni.**
Agricultural Land	0	3.824762	2.461671	12.19	87.81
Grassland	0	3.783031	2.392751	18.82	81.18
Shrubland	-0.35267	4.081514	2.426563	20.52	79.48
Bareland	-0.51108	4.015801	2.149265	32.22	67.78
Dense woodland	0	3.840867	2.436009	18.5	81.5
Forest	0	3.557715	2.415256	20.3	79.7
Awash Basin	-0.511076	4.081514	2.336993	22.44	77.56
2. Theil-Sen Slope					
Land Cover Types	**MIN**	**MAX**	**MEAN**	**Rate Change Yr^{-1}**	
Agricultural Land	0	1.607133	0.892227	10.70672	
Grassland	0	1.429974	0.715481	8.585772	
Shrubland	-0.0412	1.434772	0.54934	6.59208	
Bareland	-0.07578	1.254819	0.374343	4.492116	
Dense woodland	0	1.451367	0.670226	8.042712	
Forest	0	1.577876	0.624232	7.490784	
Awash Basin	0.101551	1.388509	0.688178	8.258141	

4.3. NDVI in Response to Rainfall Variability

There is a time lag between rainfall events and response of vegetation event. The time interval between rainfall event and the time when precipitated water might reach a plant root and affect plant growth can vary from 1 to 12 weeks depending on vegetation types (Li et al., 2002). Correlation coefficient between calculated NDVI (monthly maximum, mean annual and annual maximum NDVI and rainfall has been computed for the time lags of 0, 1, and 2 months to identify the strongest relationship among them.

The pattern and response of NDVI in all land cover classes nearly showed similar patterns by following the main rainfall season. However, as it was described by Zhong et al (2010) the lag between precipitation and NDVI was more complicated though in most cases NDVI lagged one

to three months behind precipitation. Eklundh (1996) had investigated the lag of NDVI from precipitation in East Africa and described that one month lag was most frequent occurrence in most parts of the region.

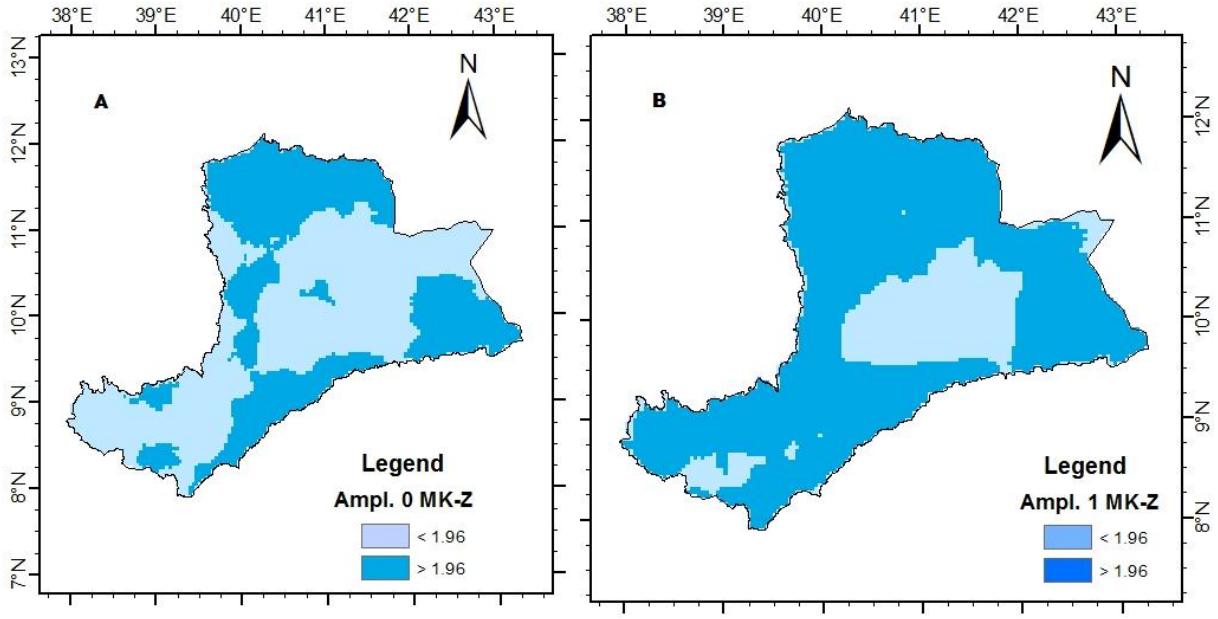

Figure 4.6 Rainfall seasonal trend of CMK amplitude 0 (A) and amplitude 1 (B)

Long- term monthly maximum NDVI and rainfall correlation for five major classes of land use namely agricultural land, grassland, shrubland, dense woodland and forests were analyzed. Table 4.9 contains these correlations. It is observed that monthly maximum NDVI and rainfall correlation values in shrubland, agricultural land and grasslands have highest maximum correlation of 0.73, 0.72 and 0.70 at lag1, but the highest mean correlation values in lag1 are 0.45, 0.44 and 0.42 for agricultural land, grassland and dense woodlands. It is also evident from table 4.7; agricultural land has better mean correlation than other land cover classes in lag2, but weak correlation than lag1.

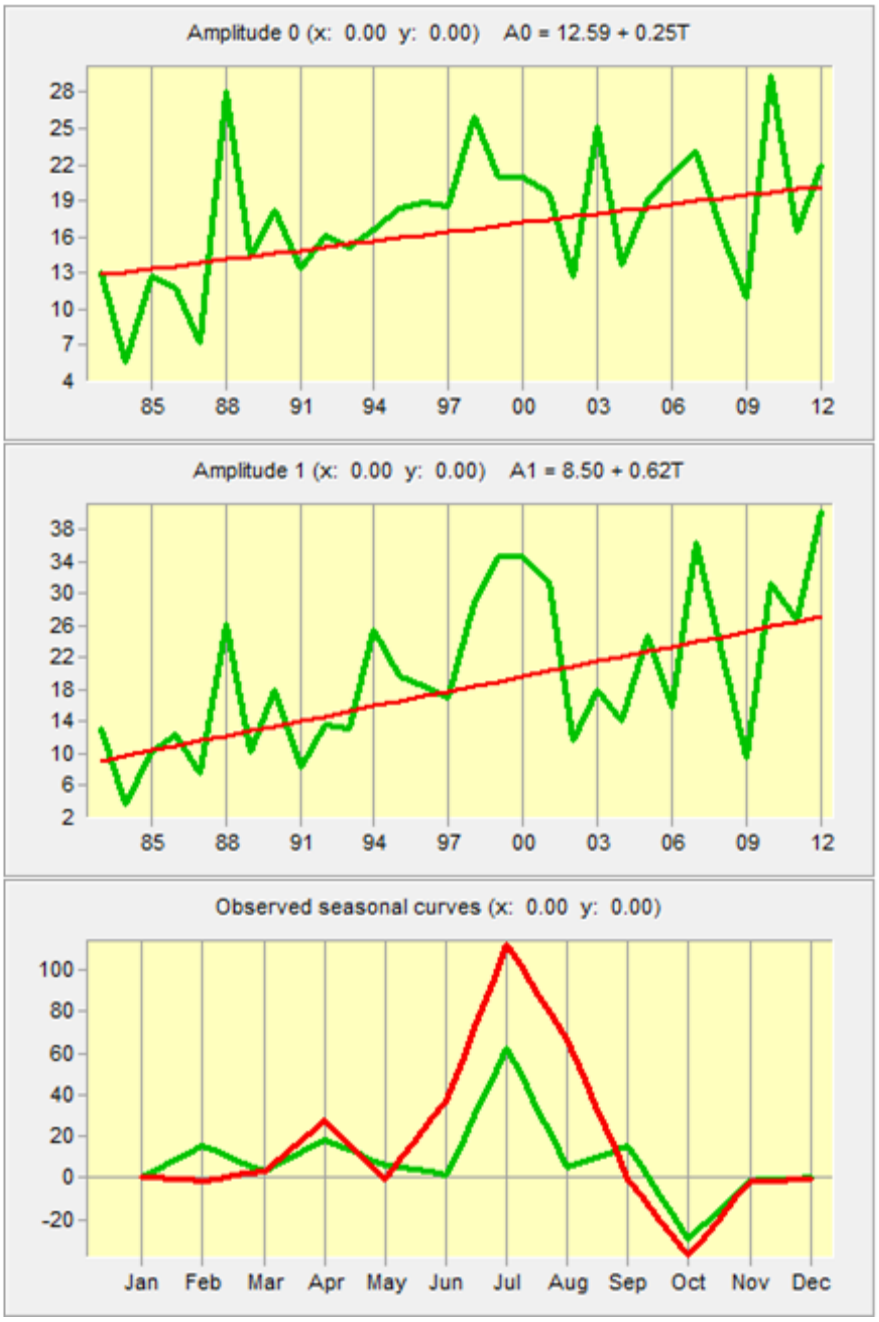

Figure 4.7 Seasonal RFE of amplitude 0 (upper), amplitude 1 (middle) and observed seasonal curves (bottom)

Table 4.9: Monthly maximum NDVI/rainfall correlation coefficients for different land cover/use types

Vegetation Type	Lag_0		Lag+1		Lag+2	
	Max	Mean	Max	Mean	Max	Mean
Agricultural Land	0.42	0.06	0.73	0.45	0.66	0.33
Grassland	0.42	0.17	0.71	0.44	0.58	0.18
Shrub Land	0.43	0.17	0.73	0.39	0.65	0.09
Bareland	0.43	0.14	0.71	0.37	0.56	0.05
Dense Woodland	0.38	0.14	0.61	0.42	0.51	0.17
Forest	0.38	0.04	0.61	0.36	0.59	0.23

Lag0, lag1 and lag2 indicates same, one month and two month

Moreover, the monthly maximum NDVI and rainfall correlation of highest values are observed for all land use types with one month time lag of rainfall. On the other hand, agricultural land (rainfed crop) has better mean correlation than others. This indicates that, the short period of rainfall dependent crop lands have shallow root and respond more quickly for seasonal rainfall than other deep rooted plants. This is consistent with the adaptive strategies used by plants to use water efficiently as deep rooted plants are more buffered from climatic fluctuations than from shallow rooted crop plants (Wang et al., 2004; as cited in Chopra, 2006). Thus time lag one can be considered as a good indicator of monthly maximum NDVI and rainfall relation in the study area.

The other correlation coefficient was computed for the long term annual maximum NDVI-rainfall relationship. This is important to understand the long term time series inter-annual relationship. It can be observed from table 4.10 and Figure 4.8, bareland, grassland, agricultural land and shrubland have highest maximum correlation coefficient of 0.85, 0.84, 0.78 and 0.75; whereas their mean correlation values are 0.24, 0.24, 0.24 and 0.30 at lag0. Moreover, at lag1 and 2 low annual maximum NDVI-rainfall correlations have been observed with slight better relationship for the maximum correlation value and poor relationship for mean correlation value. This indicates that, lag0 have better correlation for maximum annual NDVI/rainfall relationship

at the study area. Therefore, long-term inter-annual interval at lag0 i.e. less than a month can be considered as an indicator for NDVI and rainfall relationship for Awash basin.

Table 4.10 Maximum annual NDVI/rainfall correlation coefficients for different land cover/use types

Vegetation Type	Lag_0		Lag+1		Lag+2	
	Max	Mean	Max	Mean	Max	Mean
Agricultural Land	0.78	0.24	0.58	0.08	0.57	0.00
Grassland	0.75	0.31	0.49	-0.01	0.49	-0.01
Shrub Land	0.84	0.25	0.59	-0.06	0.50	-0.04
Bareland	0.85	0.24	0.68	-0.11	0.58	-0.04
Dense Woodland	0.74	0.22	0.58	0.02	0.41	-0.02
Forest	0.67	0.19	0.42	0.07	0.41	-0.03

Table 4.11 Mean annual NDVI-rainfall correlation coefficients for different land cover/use types

Land Cover Type	Lag_0		Lag+1		Lag+2	
	Max	Mean	Max	Mean	Max	Mean
Agricultural Land	0.24	-0.05597	0.56468	0.281025	0.494099	0.239897
Grassland	0.22	0.038641	0.521704	0.293465	0.468264	0.161432
Shrub Land	0.25	0.039275	0.546455	0.203469	0.496981	0.11088
Bareland	0.23	0.039275	0.557711	0.147997	0.423936	0.074274
Dense Woodland	0.17	0.004727	0.486232	0.256565	0.464422	0.141396
Forest	0.18	-0.05233	0.415564	0.190116	0.413622	0.160214

If we look at table 4.11, it can be concluded that all land cover types have better correlation coefficient at lag1 than lag0 and lag2. It can be also observed that agricultural land, shrubland and grassland have highest maximum correlation coefficient of 0.56, 0.54 and 0.52 in lag1. However, mean correlation coefficient for grassland (0.29), agricultural land (0.28) and dense

woodland (0.25) in lag1. This reveals that, lag1 can be considered as an indicator for vegetation green up responded better after one month rainfall in the study area.

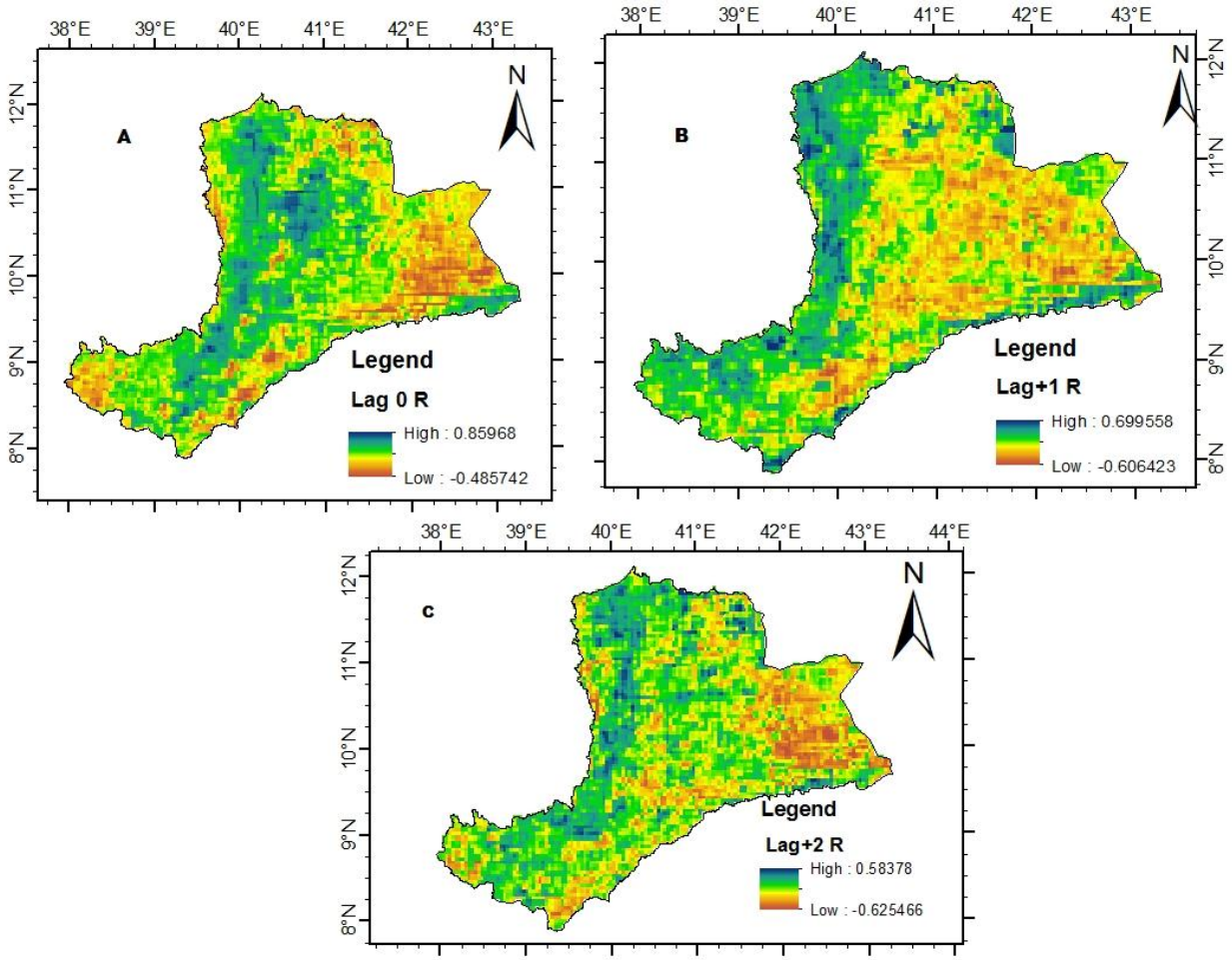

Figure 4.8: Long-term annual maximum NDVI-rainfall correlations at lag0 (A), lag1 (B), lag2 (C)

CHAPTER FIVE

CONCLUSION AND RECOMMENDATION

5.1 Conclusion

This study has been conducted to assess the spatio-temporal patterns of NDVI in response to rainfall variability from 1983 to 2012 in Awash basin Ethiopia by using satellite derived data from NOAA-AVHRR GIMMS NDVI3g and TAMSAT RFE. Based on the results of the study, the following conclusions have been derived;

The results from these two data sets have revealed the spatial and temporal patterns of rainfall and vegetation is in agreement with the results from different studies in the study area.

The results from the seasonal trend analysis of the spatial and temporal patterns of NDVI as well as the response of NDVI to rainfall variability indicates that, the time where NDVI and rainfall become the lowest and the highest can tell as the dry and wettest seasons; consequently an indicators of drought and flood. This indicates that, the NOAA-AVHRR GIMMS NDVI3g can be used for early warning system.

Finally, for short term lag relationship, maximum monthly NDVI in response to rainfall variability has resulted better correlation at lag1 (30 days) and can be taken as an indicator for the response of vegetation for rainfall in the study area; whereas for long term lag relationship mean annual NDVI-rainfall correlation at lag0 (less than 30 days) where vegetation better respond for rainfall in Awash basin.

5.2. Recommendation

- This study has used satellite data 15 days MVC of GIMMS NDVI3g at 8 km spatial resolution and monthly TAMSAT RFE at 4 kilometer spatial resolution. Therefore, it is important for future researches to conduct a study with better resolution and ground based data to better understand the spatio-temporal patterns as well as the lag relationship of vegetation in response to rainfall variability.
- Different factors should be considered for the long term decreasing and increasing trend of vegetation and rainfall so as to conclude the seasonal and long term relationship.
- The findings of this study will be used for early warning system by the stakeholders of both governmental and non-governmental organizations.

References

Anyambaa, B., and Tucker, C.J. (2005). Analysis of Sahelian vegetation dynamics using NOAA-AVHRR NDVI data from 1981–2003. Journal of Arid Environments, 63; 596–614.

Asadullah, A., McIntyre, N., and Kigobe, M. (2008). Evaluation of five satellite products for estimation of rainfall over Uganda. Hydrol. Sci. J., 53, 1137–1150, doi:10.1623/hysj.53.6.1137.

Atkinson, P.M., Jeganathan, C., Dash, J., and Atzberger, C. (2012). Inter-comparison of four models for smoothing satellite sensor time-series data to estimate vegetation phenology. *Remote Sens.Environ*, *123*, 400–417.

Atzberger, C. and Eilers, P.H.C., (2011). A time series for monitoring vegetation activity and phenology at 10-daily time steps covering large parts of South America. *Int. J. Appl. Earth Obs. Geoinf.*,*4*:365–386.

Atzberger, C., (2013). Advances in remote sensing of agriculture: Context description, existing operational monitoring systems and major information needs. *Remote Sens*, *5*, 949–981.

Belayneh, A., Adamowski, J., Khalil, B., and Ozga-Zielinski, B. (2013). Long-term SPI drought forecasting in the Awash River Basin in Ethiopia using wavelet neural network and wavelet support vector regression models. Journal of Hydrology, 508(2014); 418-429.

Beurs, K. M. and Henebry, G. M. (2005). A statistical framework for the analysis of long image time series, International Journal of Remote Sensing, 26(8), (1551-1573). DOI: 10.1080/01431160512331326657

ChamailléJammes A.B., and Fritz H. (2009). Precipitation–NDVI relationships ineastern and southern African savannasvary along a precipitation gradient. International Journal of RemoteSensing 30:13, 3409-3422. DOI: 10.1080/01431160802562206

Central Statistical Agency (CSA), (2007). Population census of the Federal Democratic Republic of Ethiopia. Central Statistical Authority, Addis Ababa, Ethiopia.

Chopra, P. (2006). Drought Risk Assessment using Remote Sensing and GIS: A case study of Gujarate. A Thesis Submitted to the International Institute for Geo-Information Science and Earth Observation in partial fulfillment of the requirement for the degree of Master of Science in Geo-information Science and Earth Observation in Hazard and Risk Analysis.

Cochrane D., and Orcutt G.H. (1949). Application of Least Squares Regression to Relationships Containing Auto-correlated Error Terms. *J Amer Statistical Assoc.* 44: 32-61.

Cracknell, A.P. (2001). The exciting and totally unanticipated success of the AVHRR in applications for which it was never intended. *Adv. Space Res.*, *28*, 233–240.

Deering, D.W. (1978). Rangeland Reflectance Characteristics Measured by Aircraft and Spacecraft Sensors. Ph.D. Thesis, Texas A & M University, College Station, TX, USA.

Desalegn. C., Babel, M.S., Das Gupta, A., Seleshi, B.A., & Merrey, D. (2006). Farmer's perception about water management under drought conditions in the Awash River Basin, Ethiopia. International Journal of Water Resources Development 22 (4), 589 – 602

Desalegn, C., Babel. M.S., and Gupta, A.D. (2010). Drought Analysis on the Awash River Basin, Ethiopia. Water Resources Management, 24, 1441 – 1460.

Donald W. M., Spooner, J., Steven A. D., and Jon B. Harcum J.B., (2011). Statistical Analysis for Monotonic Trends. Tech Notes 6, Developed for U.S. Environmental Protection Agency. Retrived from:*www.bae.ncsu.edu/programs/extension/wqg/319monitoring/tech_notes.htm*

Eastman, J.R., Florencia S., Bardan G., Honglei Z., Hao C., Neeti N., Yongming C., Elia A. M. & Stefano C. C. (2009). Seasonal trend analysis of image time series, International Journal of Remote Sensing, 30(10), 2721-2726, DOI: 10.1080/01431160902755338

Eastman, R. (2016). Terrset manual. Clarklabs, Clark University.

Eklundh, L. (1996). AVHRR NDVI for Monitoring and mapping of vegetation and drought in East African environments. Doctoral Dissertation. Lund University Press.

Teferi, E., Uhlenbrook, S., and Weldeamlak, B. (2015). Inter-annual and seasonal trends of vegetation condition in the Upper Blue Nile (Abbay) basin: dual scale timeseries analysis. Earth Syst. Dynam. Discuss., 6, 169–216. doi:10.5194/esdd-6-169-2015

Esubalew N. (2014). GIS and Remote Sensing the spatio-temporal climate variability analysis the case of Ziway Dugda and Dodota woreda, arsi zone, Oromia region, Ethiopia. A master thesis in Geography and Environmental Studies Specialization in Geographic Information System (GIS), Remote Sensing (RS), and Digital Cartography Addis Ababa University, Addis Ababa, Ethiopia

Fabricante, I., Oesterheld, M., Paruelo, J.M. (2009). Annual and seasonal variation of NDVI explained by current and previous precipitation across Northern Patagonia. Journal of Arid Environments, 73: 745–753.

Food and Agricultural Organization (FAO), (2014). Remotely sensed information for crop monitoring and food security – techniques and methods for arid and semi-arid areas. E-learning to meet the needs of agriculture and food security professionals.

George, A. and Hanuschak, S. (2010). Timely and accurate crop yield forecasting and estimation, history and initial gap analysis.

Getahun Y. S., and Shafin, B.G. (2015). Analysis of Climate Variability (ENSO) and Vegetation Dynamics in Gojjam, Ethiopia. J Earth SciClim Change, 6:10.

http://dx.doi.org/10.4172/2157-7617.1000320

Getahun T. (2012). Assessment of spatio-temporal patterns of NDVI in response to precipitation using NOAAAVHRR rainfall estimate and NDVI data from 1996-2008, Ethiopia.Master's thesis Physical Geography and Quaternary Geology, Stockholm University.

Getinet. F. (2010). Comparative Analysis of Climate Variability and Impacts in Central Rift Valley and Adjacent Arsi Highlands Using GIS and Remote Sensing. M.sc thesis, Addis Ababa University, Addis Ababa, Ethiopia.

Gezahegn N. (2016). Spatial Assessment of NDVI as an Indicator of Desertification in Ethiopia using Remote Sensing and GIS. Master Thesis in Geographical Information Science Department of Physical Geography and Ecosystem Science Centre for Geographical Information Systems Lund University, Lund Sweden.

Gutman G. and Ignatov, A. (1998). The derivation of the green vegetation fraction from NOAA/AVHRRdata for use in numerical weather prediction models. int. j. remote sensing,19(8), (1533-1543).

Halcrow, (2006). Awash river basin flood control and watershed management study project. Halrow and MoWE, Addis Ababa, Ethiopia.

Herman, A., Kumar, V. B. B., Arkin, P. A, and Kousky, J. V. (1997). Objectively determined 10-day African rainfall estimates created for famine early warning systems. Int. J. Remote Sens., 18, 2147–2159, doi:10.1080/014311697217800.

Hird, J.N., and McDermid, G.J. (2009). Noise reduction of NDVI time series: An empirical comparison of selected techniques. *Remote Sens. Environ.,113*, 248–258.

Hoaglin, D.C., Mosteller, F., and Tukey, J.W. (2000). Understanding Robust and Exploratory Data Analysis, Wiley Classics Library Edition, (New York: Wiley).

Holben, B. N. (1986). Characteristics of maximum-value composite images from temporal AVHRR data, Int. J. Remote Sens., 7, 1417– 1434.

Huete A, Justice, C., and Liu, H. (1994). Development of vegetation and soil indexes for MODIS-EOS. Remote Sens.Environ. 49(224-234).

Intergovernmental Panel on Climate Change (IPCC), (2007). *Climate change 2007*: Impacts, Adaptation and Vulnerability. Working Group II contribution to the Intergovernmental Panel on Climate Change Fourth Assessment Report: summary for Policymakers. Cambridge University Press, Cambridge, UK.

Jackson, R.D., and Huete, R. (1991). Interpreting vegetation indices. Preventive veterinary medicine, Elsevier Science Publisher, Amsterdam, 11(185-200).

Jensen, J.R. (1996). Introductory Digital Image Processing. 2nded, Englewood Cliffs, NY: Prentice-Hall.

Jobard, I., Chopin, F., Berges, J., & Roca, R. (2011). An intercomparison of 10-day satellite precipitation products during West African monsoon. Int. J. Remote Sens., 32, 2353–2376, doi:10.1080/01431161003698286.

Kenawy, A.M.El., Mccabe, M.F., Vicente-Serrano, S.M., Lopez-Moreno, J.I., Robaa, S.M. (2016). Changes in the frequency and severity of hydrological droughts over Ethiopia from 1960 to 2013. CIG 42(1), p. 145-166.

Kaufmann, R.K., Zhou, L., Knyazikhin, Y., Shabanov, N.V., Tucker, C.J. (2000). Effect of orbital drift and sensor changes on the time series of AVHRR vegetation index data. *IEEE Trans. Geosci.Remote Sens.*, 38, 2584–2597.

Laurent, H., Jobard, I., and Toma, A. (1998). Validation of satellite and ground-based estimates of precipitation over the Sahel. Atmos. Res., 47-48, 651–670. doi:10.1016/S0169-8095(98)00051-9.

Leilei, L., Jianrong, F., & Yang, C. (2014).The relationship analysis of vegetation cover, rainfall and land surface temperature based on remote sensing in Tibet, China. IOP Conf. Series: Earth and Environmental Science. doi:10.1088/1755-1315/17/1/012034

Li, B., Tao, S., et al., (2002). Relations between AVHRR NDVI and ecoclimatic parameters in China. International Journal of remote Sensing, Vol.23(No.5): 989-999.

Lillesand, T.M, Kiefer, R. and Chipman, J.W. (2004). Remote Sensing and Image Interpretation (5th edition).John Wiley & sons, Inc. New York.

Maidment, R. I., D. I. F. Grimes, R. P. Allan, H. Greatrex, O. Rojas, and O. Leo, (2013). Evaluation of satellite-based and model re-analysis rainfall estimates for Uganda. Meteor. Appl., 20, 308–317, doi:10.1002/met.1283.

Maidment, R. I., D. Grimes, Allan R. P., Tarnavsky E., M. Stringer, T. Hewison, R. Roebeling, and Black E., (2014). The 30 year TAMSAT African Rainfall Climatology and Time series (TARCAT) data set. J. Geophys. Res. Atmos., 119(10);619–644. DOI:10.1002/ 2014JD021927.

Martiny, N., Camberlin, P., Richard, Y and Philipon, N. (2006). Compared regimes of NDVI and Rainfall in Semi-arid regions of Africa, international Journal of Remote Sensing, 27 (23-24), (5201-5223).

Mekonnen, D., (2016). Studies on Temporal Relationship between Normalized Difference Vegetation Index and Rainfall in the Southern Part of Ethiopia. Journal of Environment and Earth Science. 6(6), 93-97.

Miguel A., Campo-Bescós R., Muñoz, C., Jane, S., Likai, Z.,Peter R. W., & Erin B. (2013). Combined Spatial and Temporal Effects of EnvironmentalControls on Long-Term Monthly NDVI in the SouthernAfrica Savanna. Remote Sens., 5.

Milford, J.R., Mcdougall, V.D., &Dugdale, G., (n.d). Rainfall estimationfrom cold cloud duration:experience of the TAMSAT group in West Africa. Department of Meteorology, University of READING, U.K.

Mingjun, D., Yili, Z., Linshan, L., Wei, Z., Zhaofeng, W., Wanqi, B. (2007). The relationship between NDVI and precipitationon the Tibetan Plateau, *Journal of Geographical Sciences* DOI: 10.1007/s11442-007-0259-7

National Meteorological Agency (NMA), (2007). *National Adaptation Program of Action of Ethiopia (NAPA)*. National Meteorological Agency, Addis Ababa, Ethiopia.

Neeti, N. & Eastman, R. (2011). A contextual Mann-Kendall approach for the assessment of trend significance in image time series. Transactions in GIS, 15(5): 599-611.

NEST, 2003. Climate Change in Nigeria: A Communication Guide.

Nicholson S.E., Davenport. M.L., Malo A.R. (1990). The comparison of the vegetation response to rainfall in the Sahel and East Africa, using normalized difference vegetation index from NOAA AVHRR. Climatic Change 17: 209-241.

Pinzon, J.E. & Tucker, C.J., (2014). A non-stationary 1981–2012 AVHRR NDVI3g Time Series. *Remote Sens., 6,* 6929-6960. doi:10.3390/rs6086929

Obasi, G.O.P., (2003b). Regional conference on climate change and food Sustainability in the 21st century: Keynote Address, Lagos, Nigeria, 11.

Rembold, F., Atzberger, C., Savin, I., & Rojas O. (2013). Using low resolution satellite imagery for yield predictionand yield anomaly detection. *Remote Sens. 5,* 1704-1733, DOI:10.3390/rs5041704.

Roerink, G.J., Menenti, M., and Verhoef, W. (2000). Reconstructing cloud free NDVI composites using Fourier analysis of time series, International Journal of Remote Sensing.

Rouse, J. W. Jr., Haas, R., H., Deering, D. W., Schell, J. A., & Harlan, J. C., 1974. Monitoring the vernal advancement and retrogradation (Green Wave Effect) of Natural Vegetation. *NASA/GSFC Type III Final Report*, Greenbelt, MD., 371.

Rousvel. S., Armand N, Andre L., Tengeleng S.,Alain, T. S. (2013). Comparison between vegetation and rainfall of bioclimatic ecoregions in Central Africa. *Atmosphere,* 4,11-427; doi:10.3390/atmos4040411

Sellers, P.J. (1985). Canopy reflectance, photosynthesis and transpiration. *Int. J. Remote Sens,6:*1335–1372.

Shiferaw A. (2011). Evaluating the land use and land cover dynamics in BorenaWoreda of South Wollo highlands, Ethiopia. J Sustainable Development in Africa 13: 87-107.

Shisanya, C. A., Recha, C., &Anyamba, A. (2011). Rainfall variability and its impact on normalizeddifference vegetation index in arid and semi-aridlands of Kenya. *International Journal of Geosciences.* 2, 36-47. doi:10.4236/ijg.2011.21004.

Snijders, F. J. (1991). Rainfall monitoring based on Meteosat data—A comparison of techniques applied to the western Sahel. Int. J. Remote Sens., 12, 1331–1347.

Tarnavsky E., Grimes D., Maidment R., Black E.,. Allan R.P., & Stringer M. (2014). Extension of the TAMSAT satellite-based rainfall monitoring over Africa and from 1983 to present. J.App.Meteo. and Clim. 53, 2805-2882. DOI: 10.1175/JAMC-D-14-0016.1

Thiam A. and Eastman, J.R. (n.d.). Terrset Mannual. Clark labs, Ronald Eastman pp:186-196.

Thiam, A.K. (1997). Geographic information systems and remote sensing methods for assessing and monitoring land degradation in the Sahel: The Case of Southern Mauritania. Doctoral Dissertation, Clark University, Worcester Massachusetts.

Thorne, V., Coakeley, P., Grimes, D., &Dugdale, G. (2001). Comparison of TAMSAT and CPC rainfall estimates with raingauges, for southern Africa. Int. J. Remote Sens., 22, 1951–1974, doi:10.1080/01431160118816.

Tucker, C.J., Vanpraet, C., Boerwinkel, E., Gaston, A. (1980). Satellite remote sensing of total dry matter production in the Senegalese Sahel. *Remote Sens. Environ,13:* 461–474.

Tucker, M. R., & Sear, C. B. (2001). A comparison of Meteosat rainfall estimation techniques in Kenya. Meteor. Appl., 8, 107– 117, doi:10.1017/S1350482701001098.

Tufa D., (2007). Use of satellite rainfall estimates for improving climate services in Africa. International Research Institute for Climate and Society (IRI); the Earth Institute at Columbia University.

Tufa D., Kinfe H., Ross M., Tarnavsky, E., & Connor S. (2014). Combined use of satellite estimates and rain gaugeobservations to generate high-quality historical rainfall timeseries over Ethiopia. *Int. J. Climatol.* 34: 2489–2504. DOI: 10.1002/joc.3855

Udelhoven, T., Stellmes, M., Del-Barrio, G., & Hill, J. (2005). NDVI - Rainfall relationships for 1989 to 1999 for Spain**.** *International Journal of Remote Sensing*.

United Nations Framework Convention on Climate Change (UNFCC), (2010). Climate change: impacts, vulnerabilities and adaptation in developing countries. United Nations Framework Convention on Climate Change (UNFCCC), Climate Change Secretariat pp: 68.

USAID (2006). Agro-Climatic Monitoring. Famine Early Warning Systems Network (FEWSNET). Retrieved from http://www.fews.net/pages/imageryhome.aspx?pageID=Ndvi

Vermote, E.F., & Kaufman, Y.J. (1995). Absolute calibration of AVHRR visible and near-infrared channels using ocean and cloud views. *Int. J. Remote Sens.*, *16*, 2317–2340.

Vrieling A., Beurs K. M., & Brown M. E. (2011). Variability of African farming systems from phenological analysis of NDVI time series. Climatic Change, 109, 455–477. DOI:10.1007/s10584-011-0049-1

Wang, J., Rich, P. M., & Price, K.P. (2003). Temporal responses of NDVI to precipitation and temperature in the central Great Plains, USA. International Journal of Remote Sensing, 24(11), 2345-2364, DOI: 10.1080/01431160210154812

White, M.A., de Beurs, K.M., Didan, K., Inouye, D.W., Richardson, A.D., Jensen, O.P., O'Keefe, J., Zhang, G., Nemani, R.R., van Leeuwen, W.J.D.; *et al.* (2009).Intercomparison, interpretation, and assessment of spring phenology in North America estimated from remote sensing for 1982–2006. *Glob. Chang. Biol.*, *15*, 2335–2359.

Woldeamlak, B., & Conwayb, D. (2007). A note on the temporal and spatial variability of rainfall inthe drought-prone Amhara region of Ethiopia

Worku, Z. and Csaplovics, E. (2015). Assessment of rainfall and NDVI anomalies in semi-arid regions using distributed lag models. Algorithms and Technologies for Multispectral, Hyperspectral, and Ultraspectral Imagery XXI, Proc. of SPIE Vol. 9472, 94721O. doi: 10.1117/12.2176803

Yang J.S., Wang Y.Q., & August. P.V. (2011). Estimation of land surface temperature using spatial interpolation and satellite-derived surface emissivity. J Environ Informatics 4: 40-47.

Zhang, X, Friedl, M.A., Schaaf, C.B., Strahler, A.H., & Liu, Z. (2005). Monitoring the response of vegetation phenology to precipitation in Africa by coupling MODIS and TRMM instruments. J.Geophy.Res, 110.

Zhong, L., Ma, Y., Salama, M., & Su Z. (2010). Assessment of vegetation dynamics and their response to variations in precipitation and temperature in the Tibetan Plateau. Climatic change 103: 519-535.